
Apprenticeship learning with prior beliefs using inverse optimization

Mauricio Junca

*Department of Mathematics
Universidad de los Andes, Bogotá, Colombia.*

mj.junca20@uniandes.edu.co

Esteban Leiva

*Department of Industrial and Systems Engineering
University of Southern California, Los Angeles, CA, US.*

leivamon@usc.edu

Abstract

The relationship between inverse reinforcement learning (IRL) and inverse optimization (IO) for Markov decision processes (MDPs) has been relatively underexplored in the literature, despite addressing the same problem. In this work, we revisit the relationship between the IO framework for MDPs, IRL, and apprenticeship learning (AL). We incorporate prior beliefs on the structure of the cost function into the IRL and AL problems, and demonstrate that the convex-analytic view of the AL formalism emerges as a relaxation of our framework. Notably, the AL formalism is a special case in our framework when the regularization term is absent. Focusing on the suboptimal expert setting, we formulate the AL problem as a regularized min-max problem. The regularizer plays a key role in addressing the ill-posedness of IRL by guiding the search for plausible cost functions. To solve the resulting regularized-convex-concave-min-max problem, we use stochastic mirror descent (SMD) and establish convergence bounds for the proposed method. Numerical experiments highlight the critical role of regularization in learning cost vectors and apprentice policies.

Keywords: Markov Decision Processes, Apprenticeship Learning, Inverse Optimization, Stochastic Mirror Descent

1 Introduction

In scenarios where an agent must learn to navigate in a random or uncertain environment, it is a common practice to model the situation as a Markov decision process (MDP) and apply reinforcement learning (RL). The goal in RL is to find a policy that minimizes the total expected discounted cost for the agent. Usually, it is assumed that the cost function is known; however, specifying this function is difficult for most real-life scenarios (Ng & Russell, 2000). Moreover, an incorrect specification of the cost function can lead to unintended and potentially detrimental effects on the agent’s behavior (Amodi et al., 2016; Hadfield-Menell et al., 2020). Consider the problem of driving: should the agent be rewarded for arriving quickly, safely, or cheaply, and how should the importance of each factor be balanced?

Inverse reinforcement learning (IRL) tackles this problem by reducing the work of manually designing the cost function and using observations of an expert agent’s actions. Specifically, IRL aims to infer the cost function that the expert is optimizing based on recorded behavior and a model of the environment. Returning to the driving example, this approach involves observing an expert driver’s behavior and deducing the underlying objective that guides their decisions. However, the goal extends beyond identifying the cost function; in many cases, there is a desire to emulate the expert’s actions, much like a student assimilating knowledge from a mentor. For instance, when children learn to run, they are not explicitly given a cost function to optimize, but an expert shows them demonstrations of how they should run. Building on this idea, learning from demonstrations (LfD) and imitation learning (IL) seek to derive a policy that matches or surpasses the expert’s performance.

IRL was first informally proposed by Russell (1998), and Ng & Russell (2000) introduced algorithms for three scenarios: (1) when the policy, transition dynamics, and a finite state space are known; (2) when the state space is infinite; and (3) when the policy is unknown, but sample trajectories are available. Several methods have since been proposed, including a maximum margin approach (Ratliff et al., 2006), Bayesian frameworks (Ramachandran & Amir, 2007), and maximum entropy techniques (Ziebart et al., 2008). However, all of these methods rely on RL as a subroutine within an inner loop, leading to significant computational expenses.

Furthermore, the IRL problem is ill-posed (Ng & Russell, 2000), as multiple cost functions can explain an agent’s behavior. This challenge has garnered increasing attention in the literature, with several works focusing on identifying the set of feasible cost functions that account for the expert’s behavior (Metelli et al., 2021; Lindner et al., 2022). For our analysis, it is important to note that the work of Metelli et al. (2021; 2023); Lazzati et al. (2025) assumes access to a generative-model oracle for both the transition dynamics of the MDP and the expert’s policy. A key finding in this body of work is that learning the feasible cost set is inefficient and infeasible for large state spaces, as the sample complexity scales heavily with the size of the state space.

In the context of LfD or IL, the literature often adopts the apprenticeship learning (AL) formalism proposed by Abbeel & Ng (2004), which assumes access to a set of expert demonstrations and that the unknown true cost function belongs to a specific class of functions. Consequently, this assumption requires identifying a set of basis functions in advance, which can be a nontrivial task. There are two main classes of cost functions considered: (1) linear combinations of known basis functions called features (Abbeel & Ng, 2004; Syed & Schapire, 2007; Ziebart et al., 2008) and (2) convex combinations of a set of vectors (Syed et al., 2008; Kamoutsi et al., 2021). Building on the AL formalism, Syed & Schapire (2007) presented a game-theoretic view of AL and solved it using a multiplicative weights algorithm. Later, Syed et al. (2008) proposed a linear programming approach to solve the AL problem without employing IRL or RL as a subroutine. This marked an initial step toward leveraging the tools of mathematical optimization to address the LfD problem. Following this direction, Kamoutsi et al. (2021) introduced a convex-analytic approach to the LfD problem within the AL formalism using a generative-model oracle for the MDP’s transitions. They formulated a bilinear min-max problem using Lagrangian duality and solved it using stochastic mirror descent (SMD). Moreover, Ho & Ermon (2016) solved the LfD problem for a general class of cost functions, solving an entropy-regularized-min-max problem, and connected their approach with generative adversarial networks. Nevertheless, this min-max problem is nonconvex-nonconcave, limiting its theoretical understanding.

Contribution. We revisit IO’s tools for IRL and present the inverse problem for estimating the cost function of an MDP given an optimal policy (IRL-IO) (Erkin et al., 2010; Chan et al., 2023) and incorporate prior beliefs on the structure of the cost function (IRL-IO $_{\epsilon}$). Through this approach, we revisit the proof that the inverse-feasible set of this inverse problem is equivalent to the dual problem derived by Kamoutsi et al. (2021) and extend it to a general class of cost functions. Furthermore, we relax the assumption of expert optimality in (IRL-IO $_{\epsilon}$), propose a new problem tailored for suboptimal experts (IO-AL $_{\alpha}$), and characterize its optimal solution. Using Lagrangian duality, we derive a regularized-convex-concave-min-max problem (RLfD $_{\alpha}$) for solving (IO-AL $_{\alpha}$), which reduces to previous formulations (Kamoutsi et al., 2021) when the regularization term is null. Additionally, we introduce Algorithm 1 (SMD-RLfD) by showing that the stochastic mirror descent algorithm proposed in Jin & Sidford (2020) to solve ℓ_{∞} - ℓ_1 games naturally adapts to our problem, provide theoretical convergence bounds, and establish a connection between the output of SMD-RLfD and the optimal solution of (IO-AL $_{\alpha}$).

1.1 Notation

We denote the cardinality of a set \mathcal{S} as $|\mathcal{S}|$. The probability simplex over $|\mathcal{S}|$ elements is given by $\Delta^{|\mathcal{S}|} = \left\{ \mathbf{x} \in \mathbb{R}^{|\mathcal{S}|} \mid x_i \geq 0, \sum_{i=1}^{|\mathcal{S}|} x_i = 1 \right\}$ and boxes are denoted by $\mathbb{B}_b^n = \{ \mathbf{x} \in \mathbb{R}^n \mid \|\mathbf{x}\|_{\infty} \leq b \}$. The canonical basis vectors are denoted by $\mathbf{e}^i = \{ \mathbf{x} \in \mathbb{R}^n \mid e_i = 1 \text{ and } e_j = 0 \forall j \neq i \}$. The Kronecker delta is denoted by δ_{ij} . Component-wise multiplication between two vectors \mathbf{x}, \mathbf{y} is denoted by $\mathbf{x} \circ \mathbf{y}$. The nonnegative real numbers are denoted by \mathbb{R}_+ . The superscript $(\cdot)^*$ indicates optimality, for instance $\rho_{\mathbf{c}}^*$ denotes the optimal discounted expected cost of an MDP. Finally, we use the same notation as Kamoutsi et al. (2021), with minor modifications, to highlight the strong connections to their work.

2 Preliminaries and problem formulation

In this section, we establish the foundational concepts necessary for our study. We begin by defining the structure of infinite-horizon MDPs. We then introduce the IRL problem and discuss the LfD problem through the AL formalism. Finally, we provide an overview of IO and formally state our problem.

2.1 Infinite Horizon MDPs

A finite MDP is defined as a tuple $(\mathcal{S}, \mathcal{A}, P, \boldsymbol{\nu}_0, \mathbf{c}, \gamma)$ where \mathcal{S} is a finite state space, \mathcal{A} a finite action space, and P is a transition law $P = (P(\cdot | s, a))_{s,a}$ where $P(\cdot | s, a) \in \Delta^{|\mathcal{S}|}$. The initial state distribution is denoted by $\boldsymbol{\nu}_0 \in \Delta^{|\mathcal{S}|}$ and satisfies $\boldsymbol{\nu}_0(s) > 0$ for every $s \in \mathcal{S}$. The cost vector is defined as $\mathbf{c} \in \mathcal{C} \subseteq \mathbb{B}_1^{|\mathcal{S}||\mathcal{A}|}$ and the discount factor is given by $\gamma \in (0, 1)$.

A *stationary Markov policy* is a collection of distributions, indexed by $s \in \mathcal{S}$ and denoted by $(\pi(\cdot | s))_{s \in \mathcal{S}}$, where $\pi(\cdot | s) \in \Delta^{|\mathcal{A}|}$. We denote the space of stationary Markov policies by Π_0 . In this framework, the MDP begins with an initial state $s_0 \sim \boldsymbol{\nu}_0$. At each time-step t , where the current state is s_t : the agent selects an action according to $a_t \sim \pi(\cdot | s_t)$, the next state is determined by the transition law $s_{t+1} \sim P(\cdot | s_t, a_t)$, and a cost $c(s_t, a_t)$ is incurred. Note that in an infinite horizon model, the process continues indefinitely.

The *normalized value function* $\mathbf{V}_\mathbf{c}^\pi \in \mathbb{R}^{|\mathcal{S}|}$ of a policy π given a cost \mathbf{c} is given by

$$\mathbf{V}_\mathbf{c}^\pi(s) = (1 - \gamma) \mathbb{E}_s^\pi \left[\sum_{t=0}^{\infty} \gamma^t c(s_t, a_t) \right]$$

where $\mathbb{E}_s^\pi[\cdot]$ denotes the expectation with respect to the trajectories generated by π when starting from the state s . While we sometimes refer to it as a function, any function from a finite set to the reals can be naturally represented as a vector. The fundamental goal of RL is to find a policy π such that the process $((s_t, a_t))_t$ minimizes the *total expected cost*:

$$\begin{aligned} \rho_\mathbf{c}^* &= \min_{\pi \in \Pi_0} \rho_\mathbf{c}(\pi) \\ &= \min_{\pi \in \Pi_0} (1 - \gamma) \mathbb{E}_{\boldsymbol{\nu}_0}^\pi \left[\sum_{t=0}^{\infty} \gamma^t c(s_t, a_t) \right], \end{aligned} \tag{RL}_\mathbf{c}$$

where $\rho_\mathbf{c}(\pi) = \langle \boldsymbol{\nu}_0, \mathbf{V}_\mathbf{c}^\pi \rangle$. Notice that we explicitly highlight the dependence of $(\text{RL}_\mathbf{c})$ on the cost vector \mathbf{c} . Furthermore, we denote $\mathbf{V}_\mathbf{c}^*$ as the value function corresponding to the optimal policy for $\text{RL}_\mathbf{c}$.

The *normalized occupancy measure* $\boldsymbol{\mu}_\pi \in \Delta^{|\mathcal{S}||\mathcal{A}|}$ of a policy π is defined as

$$\boldsymbol{\mu}_\pi(s, a) = (1 - \gamma) \sum_{t=0}^{\infty} \gamma^t \mathbb{P}_{\boldsymbol{\nu}_0}^\pi [s_t = s, a_t = a],$$

where $\mathbb{P}_{\boldsymbol{\nu}_0}^\pi[\cdot]$ represents the probability of an event when starting from $s \sim \boldsymbol{\nu}_0$ and following π . The occupancy measure of a state-action pair can be interpreted as the discounted visitation frequency of the pair when following a particular policy. Hence, we can also write $\rho_\mathbf{c}^* = \min_{\pi \in \Pi_0} \langle \boldsymbol{\mu}_\pi, \mathbf{c} \rangle$.

We define the transition matrix $\mathbf{P} \in \mathbb{R}^{|\mathcal{S}| \times |\mathcal{S}||\mathcal{A}|}$ where $\mathbf{P}_{s',(s,a)} = P(s' | s, a)$ and the polyhedron $\mathcal{F} = \{\boldsymbol{\mu} \in \mathbb{R}^{|\mathcal{S}||\mathcal{A}|} \mid \mathbf{T}_\gamma \boldsymbol{\mu} = \boldsymbol{\nu}_0, \boldsymbol{\mu} \geq \mathbf{0}\}$ where $\mathbf{T} \in \mathbb{R}^{|\mathcal{S}| \times |\mathcal{S}||\mathcal{A}|}$, $\mathbf{T}_{s',(s,a)} = \delta_{s',s} - \gamma \mathbf{P}_{s',(s,a)}$, and $\mathbf{T}_\gamma = \frac{1}{(1-\gamma)} \mathbf{T}$. An alternative expression for \mathbf{T}_γ that is useful for computing gradient estimators is $\mathbf{T}_\gamma \boldsymbol{\mu} = \frac{1}{(1-\gamma)} (\mathbf{B} - \gamma \mathbf{P}) \boldsymbol{\mu}$ where \mathbf{B} is a binary matrix that satisfies $\mathbf{B}_{s',(s,a)} = 1$ if $s' = s$ and $\mathbf{B}_{s',(s,a)} = 0$ otherwise.

Proposition 1 (Puterman (1994)). *It holds that, $\mathcal{F} = \{\boldsymbol{\mu}_\pi \mid \pi \in \Pi_0\}$. For every $\pi \in \Pi_0$, we have that $\boldsymbol{\mu}_\pi \in \mathcal{F}$. Moreover, for every feasible solution $\boldsymbol{\mu} \in \mathcal{F}$, we can obtain a stationary Markov policy $\pi_\boldsymbol{\mu} \in \Pi_0$ by $\pi_\boldsymbol{\mu}(a | x) = \frac{\mu(x,a)}{\sum_{a' \in \mathcal{A}} \mu(x,a')}$. Then, the induced occupancy measure is exactly $\boldsymbol{\mu}$.*

Proposition 1 provides a correspondence between the elements of \mathcal{F} and occupancy measures given by stationary Markov policies. Note that the condition $\mathbf{T}_\gamma \boldsymbol{\mu} = \boldsymbol{\nu}_0$ can be interpreted as the Markov property of

the process under $\mathbb{P}_{\nu_0}^\pi[\cdot]$. Hence, the MDP linear programming approach consists of solving the (MDP-P c) problem

$$\begin{aligned} \rho_c^* &= \min_{\boldsymbol{\mu} \in \Delta^{|\mathcal{S}||\mathcal{A}|}} \langle \boldsymbol{\mu}, \mathbf{c} \rangle \\ \text{s.t. } & \mathbf{T}_\gamma \boldsymbol{\mu} = \boldsymbol{\nu}_0, \\ & \boldsymbol{\mu} \geq \mathbf{0}. \end{aligned} \tag{MDP-P c }$$

Note that the constraints enforce that $\boldsymbol{\mu} \in \mathcal{F}$, therefore an optimal $\boldsymbol{\mu}$ corresponds to an optimal policy. The corresponding dual problem is given by

$$\max_{\mathbf{u} \in \mathbb{R}^{|\mathcal{S}|}} \{ \langle \boldsymbol{\nu}_0, \mathbf{u} \rangle \mid \mathbf{c} - \mathbf{T}_\gamma^\top \mathbf{u} \geq \mathbf{0} \}, \tag{MDP-D c }$$

where an optimal \mathbf{u} represents the optimal value function V_c^* .

2.2 Inverse reinforcement learning

The IRL problem aims to uncover the true cost function that an expert agent is optimizing given some information about the expert’s behavior, for example: sample trajectories, its real policy, or an estimate of its policy (Ng & Russell, 2000). Formally, given an MDP without a cost vector and with access to information about an expert’s policy π_E , the IRL problem is defined by the tuple $(\mathcal{S}, \mathcal{A}, P, \nu_0, \pi_E, \gamma)$ and the goal is to determine a cost vector \mathbf{c} for which the policy π_E is optimal for (RL c) within the MDP $(\mathcal{S}, \mathcal{A}, P, \nu_0, \mathbf{c}, \gamma)$.

2.3 Learning from demonstrations and the apprenticeship learning formalism

The goal of learning from demonstrations is to learn a policy that matches or outperforms the expert’s policy π_E for an unknown true cost vector \mathbf{c}_{true} . The apprenticeship learning formalism (Abbeel & Ng, 2004) has been routinely used in literature for addressing the LfD problem. The AL formalism assumes that the unknown true cost function \mathbf{c}_{true} belongs to a class of functions \mathcal{C} and searches for a policy that solves the following min-max problem

$$\beta^* := \min_{\pi \in \Pi_0} \max_{\mathbf{c} \in \mathcal{C}} \langle \boldsymbol{\mu}_\pi, \mathbf{c} \rangle - \langle \boldsymbol{\mu}_{\pi_E}, \mathbf{c} \rangle = \min_{\pi \in \Pi_0} \max_{\mathbf{c} \in \mathcal{C}} \langle \boldsymbol{\mu}_\pi - \boldsymbol{\mu}_{\pi_E}, \mathbf{c} \rangle, \tag{LfD π_E }$$

An optimal solution to (LfD π_E) is called an apprentice policy π_A and satisfies

$$\langle \boldsymbol{\mu}_{\pi_A}, \mathbf{c}_{\text{true}} \rangle \leq \langle \boldsymbol{\mu}_{\pi_E}, \mathbf{c}_{\text{true}} \rangle + \beta^*.$$

In optimization-focused approaches to LfD, the \mathbf{c}_{true} is assumed to belong to a convex hull

$$\mathcal{C} = \mathcal{C}_{\text{conv}} := \left\{ \mathbf{c}_w := \sum_{i=1}^{n_c} w_i \mathbf{c}_i \mid w_i \geq 0, \sum_{i=1}^{n_c} w_i = 1 \right\}$$

(Syed et al., 2008; Kamoutsi et al., 2021) of a set of vectors $\{\mathbf{c}_i\}_{i=1}^{n_c} \subseteq \mathbb{R}^{|\mathcal{S}||\mathcal{A}|}$ where $\|\mathbf{c}_i\|_\infty \leq 1$ for each $i = 1, \dots, n_c$. It is assumed that this set of vectors is known; however, in practice, an initial estimation step is required to determine this set, a task that is generally nontrivial.

2.4 A primer on inverse optimization

Inverse optimization is a mathematical framework that fits optimization models to decision data. Given an observed optimal solution, it seeks to learn the objectives and constraints of the underlying model. For example, IRL can be thought of as an inverse optimization problem, as it searches for the cost function that an optimal agent is optimizing.

Consider the general forward optimization problem (FOP θ) for a given parameter θ in the parameter space Γ :

$$\min_{\mathbf{x} \in \mathbb{R}^n} \{ f(\mathbf{x}, \theta) \mid \mathbf{x} \in X(\theta) \}, \tag{FOP θ }$$

where $X(\theta)$ denotes the feasible set for \mathbf{x} , which depends on θ . Given an optimal solution $\hat{\mathbf{x}}$, the inverse optimization problem consists of finding a $\theta^* \in \Gamma$ that makes $\hat{\mathbf{x}}$ optimal for (FOP_θ) with $\theta = \theta^*$ and is optimal in some way. For this purpose, define the optimal solution set $X^{\text{opt}}(\theta) := \arg \min_{\mathbf{x}} \{f(\mathbf{x}, \theta) \mid \mathbf{x} \in X(\theta)\}$ and the inverse-feasible set $\Theta^{\text{inv}}(\hat{\mathbf{x}}) := \{\theta \in \Gamma \mid \hat{\mathbf{x}} \in X^{\text{opt}}(\theta)\}$. Naturally, we want to find a $\theta \in \Theta^{\text{inv}}(\hat{\mathbf{x}})$, but rather than selecting an arbitrary θ from this set, we aim for one that minimizes a certain criterion.

Hence, the inverse optimization problem (INV-OPT) is defined as:

$$\min_{\theta \in \Gamma} \{F(\theta) \mid \theta \in \Theta^{\text{inv}}(\hat{\mathbf{x}})\}, \quad (\text{INV-OPT})$$

where F should convey information about the quality of θ given some prior knowledge, and the search space Γ should be appropriately chosen for each instance of the problem.

2.5 Our problem

Suppose that the environment is modeled as an MDP where only the state space \mathcal{S} , action space \mathcal{A} , and discount factor γ are known. We assume that the learner has access to a generative-model oracle for the MDP’s transition dynamics, as well as a generative-model oracle of an expert’s occupancy measure $\boldsymbol{\mu}_{\pi_E}$ (not necessarily optimal), and a prior belief $\hat{\mathbf{c}}$ of the cost function the expert is trying to optimize for. We aim to learn a cost function \mathbf{c}_A and an apprentice policy π_A , such that π_A is optimal for $\text{RL}_{\mathbf{c}_A}$, and \mathbf{c}_A remains close to the prior $\hat{\mathbf{c}}$, while π_A performs at least as well as π_E under \mathbf{c}_A (see (IO- AL_α) below).

To address this problem, we use Algorithm 1 (SMD-RLfD), which employs the expert and transition oracles alongside the proxy cost vector $\hat{\mathbf{c}}$ to generate expected ϵ -approximate solutions of (RLfD_α) , which is the unconstrained formulation of (IO- AL_α). Hereafter, we refer to our framework as the complete process of fixing a proxy cost vector, accessing the necessary oracles, and applying SMD-RLfD to solve (RLfD_α) and obtain the resulting learned policy and cost vector.

3 The inverse optimization viewpoint

In this section, we show how the IRL problem has been addressed with the tools of IO and establish the equivalence between the AL formulation presented in Kamoutsis et al. (2021) and the inverse-feasible set of problem (IRL-IO). Afterwards, we demonstrate how prior beliefs about the structure of the cost vector can be incorporated into the IRL formulation (IRL-IO $_{\hat{\mathbf{c}}}$) and present our primary contribution: the formulation of problem (IO- AL_α) and the characterization of its optimal solution.

3.1 IRL via IO

We will use the ideas of Subsection 2.4 applied to the forward optimization problem $\text{MDP-P}_{\mathbf{c}_{\text{true}}}$, where the parameter θ corresponds to the true cost vector \mathbf{c}_{true} the expert is optimizing for. Note that we assume the existence of \mathbf{c}_{true} because the IRL problem assumes that the expert is optimal for some cost function. Therefore, let us suppose that \mathbf{c}_{true} lies in a convex class of cost functions \mathcal{C} and that the expert’s policy π_E is optimal for $\text{RL}_{\mathbf{c}_{\text{true}}}$, which means that its corresponding occupancy measure $\boldsymbol{\mu}_{\pi_E}$ is optimal for $\text{MDP-P}_{\mathbf{c}_{\text{true}}}$. The following proposition follows from complementary slackness for linear problems (Bertsimas & Tsitsiklis, 1997).

Proposition 2 (Complementary slackness). *An element $\boldsymbol{\mu}_\pi$ is an optimal solution to $(\text{MDP-P}_\mathbf{c})$ if and only if there exists a vector $\mathbf{u} \in \mathbb{R}^{|\mathcal{S}|}$ such that $\mathbf{c} - \mathbf{T}_\gamma^\top \mathbf{u} \geq \mathbf{0}$ and $\langle \boldsymbol{\mu}_\pi, \mathbf{c} - \mathbf{T}_\gamma^\top \mathbf{u} \rangle = 0$.*

Remember that \mathbf{u} is the dual variable for the equality constraint in $(\text{MDP-P}_\mathbf{c})$ and represents the value function. Therefore, the inverse-feasible set for $\boldsymbol{\mu}_{\pi_E}$ consists of the cost functions in \mathcal{C} for which such a \mathbf{u} exists

$$\Theta^{\text{inv}}(\boldsymbol{\mu}_{\pi_E}) := \{\mathbf{c} \in \mathcal{C} \mid \exists \mathbf{u} \in \mathbb{R}^{|\mathcal{S}|} : \mathbf{c} - \mathbf{T}_\gamma^\top \mathbf{u} \geq \mathbf{0}, \langle \boldsymbol{\mu}_{\pi_E}, \mathbf{c} - \mathbf{T}_\gamma^\top \mathbf{u} \rangle = 0\}.$$

Substituting for the inverse-feasible set in (INV-OPT) and choosing an appropriate function F for comparing cost vectors, we arrive to the inverse reinforcement learning problem through inverse optimization (Erkin et al., 2010; Chan et al., 2023)

$$\begin{aligned} & \min_{\mathbf{c} \in \mathcal{C}, \mathbf{u} \in \mathbb{R}^{|\mathcal{S}|}} F(\mathbf{c}) \\ \text{s.t.} \quad & \mathbf{c} - \mathbf{T}_\gamma^\top \mathbf{u} \geq \mathbf{0}, \\ & \langle \boldsymbol{\mu}_{\pi_E}, \mathbf{c} - \mathbf{T}_\gamma^\top \mathbf{u} \rangle = 0. \end{aligned} \tag{IRL-IO}$$

3.2 Connections to LfD and the AL formalism

Kamoutsi et al. (2021) considered the LfD problem under the assumption that the true cost function \mathbf{c}_{true} belongs to the convex hull $\mathcal{C}_{\text{conv}}$ of a given set of vectors. By applying an epigraphic transformation to (LfD $_{\pi_E}$), where the validity of this transformation depends on the convex hull assumption on \mathbf{c}_{true} , and deriving its dual, they arrived at the optimization problem (D $_{\pi_E}$):

$$\max_{\mathbf{c}, \mathbf{u}} \{ \langle \boldsymbol{\mu}_{\pi_E}, \mathbf{T}_\gamma^\top \mathbf{u} - \mathbf{c} \rangle \mid \mathbf{c} \in \mathcal{C}_{\text{conv}}, \mathbf{c} - \mathbf{T}_\gamma^\top \mathbf{u} \geq \mathbf{0} \}. \tag{D $_{\pi_E}$ }$$

They focus on this problem and optimize its unconstrained version derived through Lagrangian duality, where the dual variable corresponding to the constraint $\mathbf{c} - \mathbf{T}_\gamma^\top \mathbf{u} \geq \mathbf{0}$ represents the apprentice state-action visitation probability.

Theorem 1 (cf. Proposition 2 in Kamoutsi et al. (2021)). *Suppose that $\boldsymbol{\mu}_{\pi_E}$ is an optimal solution for (MDP-P $_{\mathcal{C}}$) where $\mathbf{c} \in \mathcal{C}$. Then the following equality holds:*

$$\Theta^{\text{inv}}(\boldsymbol{\mu}_{\pi_E}) = \Pi_1 \left(\arg \max_{(\mathbf{c}, \mathbf{u})} \{ \langle \boldsymbol{\mu}_{\pi_E}, \mathbf{T}_\gamma^\top \mathbf{u} - \mathbf{c} \rangle \mid \mathbf{c} \in \mathcal{C}, \mathbf{c} - \mathbf{T}_\gamma^\top \mathbf{u} \geq \mathbf{0} \} \right)$$

where Π_1 denotes the projection in the first component.

This implies that the dual problem (D $_{\pi_E}$) serves as an alternative representation of the inverse-feasible set $\Theta^{\text{inv}}(\boldsymbol{\mu}_{\pi_E})$. In contrast, in problem (IRL-IO) we choose an element within the inverse-feasible set that minimizes F . In this sense, under the assumption of expert's optimality and that $\mathbf{c}_{\text{true}} \in \mathcal{C}_{\text{conv}}$, the AL formalism finds an arbitrary element of the inverse-feasible set, whereas (IRL-IO) has a criterion for searching within this space and considers a general convex class of cost functions \mathcal{C} .

3.3 Incorporating prior beliefs

Suppose we are given a proxy cost vector $\hat{\mathbf{c}}$ that reflects our prior beliefs about the structure of the true cost vector, which are not necessarily accurate. Leveraging this information, we aim to guide the search within the inverse feasible set in problem (IRL-IO). To this end, we project $\hat{\mathbf{c}}$ onto $\Theta^{\text{inv}}(\boldsymbol{\mu}_{\pi_E})$ by solving the following optimization problem:

$$\begin{aligned} & \min_{\mathbf{c} \in \mathcal{C}, \mathbf{u} \in \mathbb{R}^{|\mathcal{S}|}} \|\mathbf{c} - \hat{\mathbf{c}}\|_2^2 \\ \text{s.t.} \quad & \mathbf{c} - \mathbf{T}_\gamma^\top \mathbf{u} \geq \mathbf{0}, \\ & \langle \boldsymbol{\mu}_{\pi_E}, \mathbf{c} - \mathbf{T}_\gamma^\top \mathbf{u} \rangle = 0. \end{aligned} \tag{IRL-IO $_{\hat{\mathbf{c}}}$ }$$

Figure 1 illustrates the setting for problem (IRL-IO $_{\hat{\mathbf{c}}}$). The big polyhedral region represents the set of all occupancy measures \mathcal{F} . In particular, if we assume that the expert is optimal and the induced policy is deterministic, then $\boldsymbol{\mu}_{\pi_E}$ is a vertex of \mathcal{F} and the true cost vector \mathbf{c}_{true} , in green, is within the inverse-feasible set $\Theta^{\text{inv}}(\boldsymbol{\mu}_{\pi_E})$. The proxy cost vector $\hat{\mathbf{c}}$, in red, is not necessarily inside the inverse-feasible set and will be projected onto the inverse-feasible set by solving Problem (IRL-IO $_{\hat{\mathbf{c}}}$). This yields the cost vector closest to our prior belief that satisfies the expert's optimality conditions.

Since we are still selecting an element from the inverse-feasible set, we can derive results similar to those presented by Kamoutsi et al. (2021) for solutions to Problem (IRL-IO $_{\hat{\mathbf{c}}}$) under the assumption of expert optimality. The following corollary follows directly from the proof of Theorem 1.

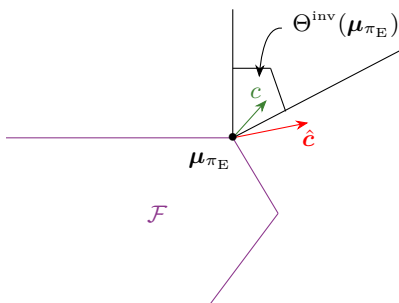


Figure 1: Illustration of (IRL-IO $_{\hat{c}}$).

Corollary 1 (Optimal expert). *Assume that π_E is optimal for (RL $_c$) with $c \in \mathcal{C}$. A pair (c_A, u_A) is optimal for Problem (IRL-IO $_{\hat{c}}$) if and only if π_E is optimal for (RL $_c$) with $c = c_A$ and $u_A = V_{c_A}^*$. In particular, the cost vector c_A is the projection of \hat{c} onto the inverse feasible set, and π_E is optimal for c_A .*

It is important to note that when the expert is suboptimal, problem (IRL-IO $_{\hat{c}}$) is infeasible, as the complementary slackness equality cannot be satisfied. To account for the possibility of suboptimal expert behavior, we can relax the complementary slackness condition in (IRL-IO $_{\hat{c}}$). Weighing the beliefs of the expert's optimality and the quality of the cost function estimate with parameter $\alpha \in \mathbb{R}_+$, we arrive to problem (IO-AL $_{\alpha}$):

$$\begin{aligned} \min_{c \in \mathcal{C}, u \in \mathbb{R}^{|\mathcal{S}|}} \quad & \alpha \|c - \hat{c}\|_2^2 + \langle \mu_{\pi_E}, c - T_{\gamma}^{\top} u \rangle \\ \text{s.t} \quad & c - T_{\gamma}^{\top} u \geq \mathbf{0}. \end{aligned} \tag{IO-AL}_{\alpha}$$

Proposition 3 (Suboptimal expert). *A pair (c_A, u_A) is optimal for (IO-AL $_{\alpha}$) if and only if the apprentice policy π_A is optimal for (RL $_c$) with $c = c_A$ and $u_A = V_{c_A}^*$. Furthermore, the optimal value corresponds to $\alpha \|c_A - \hat{c}\|_2^2 + \rho_{c_A}(\pi_E) - \rho_{c_A}(\pi_A)$.*

Proof. Observe that (IO-AL $_{\alpha}$) is a convex optimization problem. Therefore, a pair (c_A, u_A) is optimal for (IO-AL $_{\alpha}$) if and only if the KKT conditions are satisfied. In particular, it satisfies complementary slackness $\langle \mu_{\pi_A}, c_A - T_{\gamma}^{\top} u_A \rangle = 0$ and the stationarity condition $T_{\gamma} \mu_{\pi_A} = T_{\gamma} \mu_{\pi_E} = \nu_0$, which implies that $\mu_{\pi_A} \in \mathcal{F}$. Then, by Proposition 2 π_A is optimal for (RL $_c$) with $c = c_A$ and $u_A = V_{c_A}^*$. Moreover, if (c_A, u_A) are optimal we have that

$$\begin{aligned} \alpha \|c_A - \hat{c}\|_2^2 + \langle \mu_{\pi_E}, c_A - T_{\gamma}^{\top} u_A \rangle &= \alpha \|c_A - \hat{c}\|_2^2 + \langle \mu_{\pi_E}, c_A \rangle - \langle \mu_{\pi_E}, T_{\gamma}^{\top} u_A \rangle \\ &= \alpha \|c_A - \hat{c}\|_2^2 + \rho_{c_A}(\pi_E) - \langle \nu_0, u_A \rangle \\ &= \alpha \|c_A - \hat{c}\|_2^2 + \rho_{c_A}(\pi_E) - \rho_{c_A}^*. \end{aligned}$$

□

Proposition 3 states that the apprentice policy π_A , i.e., the dual variable for the constraint $c - T_{\gamma}^{\top} u \geq \mathbf{0}$, is optimal for the (RL $_c$) with cost vector c_A . Solutions to (IO-AL $_{\alpha}$) can be viewed as a way to balance the distance between the cost vector c_A and the estimate \hat{c} , while ensuring that the total expected cost of π_E and π_A are similar under c_A .

Figure 2 illustrates (IO-AL $_{\alpha}$) using the same notation as Figure 1. In this scenario, the suboptimal expert lies within the occupancy measure set \mathcal{F} rather than at a vertex. The apprentice policy π_A provides a better explanation of the expert's behavior, as it corresponds to the closest vertex, while π'_A better aligns with the proxy cost vector \hat{c} . The parameter α governs this trade-off: when α increases, the optimization problem selects $\mu_{\pi'_A}$, whereas for values closer to zero, it selects μ_{π_A} . In simple terms, α dictates the level of importance we place in our prior information versus the demonstrations provided by the suboptimal expert.

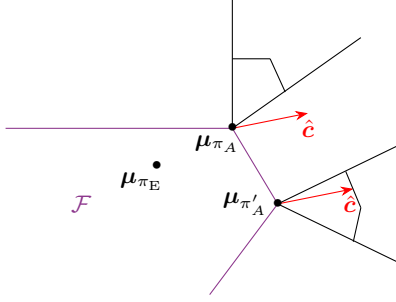


Figure 2: Illustration of (IO-AL $_{\alpha}$).

This is our alternative to the usual AL formalism: instead of identifying the set of vectors $\{\mathbf{c}_i\}_{i=1}^{n_c}$ that define $\mathcal{C}_{\text{conv}}$ and choosing an arbitrary cost vector within the inverse-feasible set, we search over a general convex class of cost vectors \mathcal{C} and define an estimate $\hat{\mathbf{c}}$ to guide the search. In practice, obtaining information about optimal experts is challenging (Brown et al., 2019; Chen et al., 2021; Wang et al., 2021), and given an expert’s policy or demonstrations, it is difficult to determine whether it is optimal. Nonetheless, we still aim to leverage suboptimal experts’ information and comprehend its actions by solving IO-AL $_{\alpha}$.

3.4 Min-max formulation

We aim to reformulate (IO-AL $_{\alpha}$) as a convex-concave-min-max problem and solve this unconstrained optimization problem using stochastic mirror descent. To this end, we compute its Lagrangian:

$$\mathcal{L}(\mathbf{c}, \mathbf{u}, \boldsymbol{\mu}) = \alpha \|\mathbf{c} - \hat{\mathbf{c}}\|_2^2 + \langle \boldsymbol{\mu}_{\pi_E} - \boldsymbol{\mu}, \mathbf{c} - \mathbf{T}_{\gamma}^{\top} \mathbf{u} \rangle$$

where $\boldsymbol{\mu} \in \mathbb{R}^{|\mathcal{S}||\mathcal{A}|}$ and $\boldsymbol{\mu} \geq \mathbf{0}$. Observe that $\mathcal{L}(\mathbf{c}, \mathbf{u}, \boldsymbol{\mu})$ is convex on (\mathbf{c}, \mathbf{u}) and concave on $\boldsymbol{\mu}$. Thus, (IO-AL $_{\alpha}$) is equivalent to the min-max problem

$$\min_{\mathbf{c} \in \mathcal{C}, \mathbf{u} \in \mathbb{R}^{|\mathcal{S}|}} \max_{\boldsymbol{\mu} \geq \mathbf{0}} \mathcal{L}(\mathbf{c}, \mathbf{u}, \boldsymbol{\mu}).$$

In our setting, we assume that $\mathcal{C} = \mathbb{B}_1^{|\mathcal{S}||\mathcal{A}|}$, which is not restrictive because we can scale any cost vector to lie within this set. Therefore, we know that $\|\mathbf{V}_{\mathbf{c}}^{\pi}\|_{\infty} \leq 1$ for any policy $\pi \in \Pi_0$ and $\mathbf{c} \in \mathcal{C}$ (see Lemma 3 in the Appendix). Hence, we can search for (\mathbf{c}, \mathbf{u}) within the box $\mathbb{B}_1^{|\mathcal{S}||\mathcal{A}|} \times \mathbb{B}_1^{|\mathcal{S}|}$. Moreover, as all feasible solutions for (MDP-P $_{\mathcal{C}}$) belong to the simplex $\Delta^{|\mathcal{S}||\mathcal{A}|}$, we can restrict the search for $\boldsymbol{\mu}$ to the same simplex.

$$\min_{(\mathbf{c}, \mathbf{u}) \in \mathbb{B}_1^{|\mathcal{S}||\mathcal{A}|} \times \mathbb{B}_1^{|\mathcal{S}|}} \max_{\boldsymbol{\mu} \in \Delta^{|\mathcal{S}||\mathcal{A}|}} \alpha \|\mathbf{c} - \hat{\mathbf{c}}\|_2^2 + \langle \boldsymbol{\mu}_{\pi_E} - \boldsymbol{\mu}, \mathbf{c} - \mathbf{T}_{\gamma}^{\top} \mathbf{u} \rangle. \quad (\text{RLfD}_{\alpha})$$

Observe that this formulation closely resembles previous min-max formulations of the LfD problem (Kamoutsi et al., 2021). It can be interpreted as a regularized version of this problem, where the search for \mathbf{c} is conducted within a general class of cost functions rather than being restricted to a previously specified convex hull.

4 Algorithm

Revisiting the assumptions for our problem, we assume that we have access to a generative-model oracle of the expert’s occupancy measure $\boldsymbol{\mu}_{\pi_E}$, as well as a generative-model oracle for the MDP’s transition law. In this section, we will focus on solving (RLfD $_{\alpha}$) via stochastic mirror descent. Before attempting to solve this problem, we must first define what constitutes a good solution. We define an ϵ -approximate solution as a pair $(\mathbf{c}, \mathbf{u}), \boldsymbol{\mu}$ such that their duality gap is bounded by $\epsilon > 0$.

Definition 1 (ϵ -approximate solution). *Given $\epsilon > 0$, an ϵ -approximate solution of (RLfD $_{\alpha}$) is a pair of feasible solutions $((\mathbf{c}^{\epsilon}, \mathbf{u}^{\epsilon}), \boldsymbol{\mu}^{\epsilon}) \in \left(\mathbb{B}_1^{|\mathcal{S}||\mathcal{A}|} \times \mathbb{B}_1^{|\mathcal{S}|}\right) \times \Delta^{|\mathcal{S}||\mathcal{A}|}$ that satisfy*

$$\text{Gap}((\mathbf{c}^{\epsilon}, \mathbf{u}^{\epsilon}), \boldsymbol{\mu}^{\epsilon}) := \max_{\boldsymbol{\mu}' \in \Delta^{|\mathcal{S}||\mathcal{A}|}} \mathcal{L}((\mathbf{c}^{\epsilon}, \mathbf{u}^{\epsilon}), \boldsymbol{\mu}') - \min_{(\mathbf{c}', \mathbf{u}') \in \mathbb{B}_1^{|\mathcal{S}||\mathcal{A}|} \times \mathbb{B}_1^{|\mathcal{S}|}} \mathcal{L}((\mathbf{c}', \mathbf{u}'), \boldsymbol{\mu}^{\epsilon}) \leq \epsilon.$$

To minimize the duality gap, we require descent and ascent directions. The gradients of $\mathcal{L}((\mathbf{c}, \mathbf{u}), \boldsymbol{\mu})$ at a given iterate $((\mathbf{c}_t, \mathbf{u}_t), \boldsymbol{\mu}_t) \in (\mathbb{B}_1^{|\mathcal{S}||\mathcal{A}|} \times \mathbb{B}_1^{|\mathcal{S}|}) \times \Delta^{|\mathcal{S}||\mathcal{A}|}$ are given by

$$\begin{aligned} g^{(\mathbf{c}, \mathbf{u})}((\mathbf{c}_t, \mathbf{u}_t), \boldsymbol{\mu}_t) &= \begin{pmatrix} 2\alpha(\mathbf{c}_t - \hat{\mathbf{c}}) + \boldsymbol{\mu}_{\pi_E} - \boldsymbol{\mu}_t \\ \mathbf{T}_\gamma \boldsymbol{\mu}_t - \mathbf{T}_\gamma \boldsymbol{\mu}_{\pi_E} \end{pmatrix}, \\ g^\mu((\mathbf{c}_t, \mathbf{u}_t), \boldsymbol{\mu}_t) &= -(-\mathbf{c}_t + \mathbf{T}_\gamma^\top \mathbf{u}_t) = \mathbf{c}_t - \mathbf{T}_\gamma^\top \mathbf{u}_t, \end{aligned}$$

where $g^{(\mathbf{c}, \mathbf{u})}((\mathbf{c}_t, \mathbf{u}_t), \boldsymbol{\mu}_t) = \nabla_{(\mathbf{c}, \mathbf{u})} \mathcal{L}((\mathbf{c}_t, \mathbf{u}_t), \boldsymbol{\mu}_t)$ and $g^\mu((\mathbf{c}_t, \mathbf{u}_t), \boldsymbol{\mu}_t) = -\nabla_{\boldsymbol{\mu}} \mathcal{L}((\mathbf{c}_t, \mathbf{u}_t), \boldsymbol{\mu}_t)$. Since explicit access to \mathbf{T}_γ and $\boldsymbol{\mu}_{\pi_E}$ is unavailable, it is necessary to develop gradient estimators that are compatible with oracle-based queries.

Definition 2 (Bounded estimator). *Given the following properties on the mean, scale, and variance of an estimator:*

1. *unbiasedness:* $\mathbb{E}[\tilde{g}] = g$.
2. *bounded maximum entry:* $\|\tilde{g}\|_\infty \leq z$ with probability 1.
3. *bounded second-moment:* $\mathbb{E}[\|\tilde{g}\|^2] \leq v$

we call \tilde{g} a $(v, \|\cdot\|)$ -bounded estimator if it satisfies 1. and 3. and a $(z, v, \|\cdot\|_{\Delta^m})$ -bounded estimator if it satisfies all conditions with local norm $\|\cdot\|_{\mathbf{w}}$ for all $\mathbf{w} \in \Delta^m$.

With this in mind, define the gradient estimator for the (\mathbf{c}, \mathbf{u}) side through the following procedure

$$\begin{aligned} \text{sample } (s, a) &\sim \frac{1}{|\mathcal{S}||\mathcal{A}|}, (s_t, a_t) \sim \boldsymbol{\mu}_t, s'_t \sim P(\cdot | s_t, a_t), \\ (s_E, a_E) &\sim \boldsymbol{\mu}_{\pi_E}, s'_E \sim P(\cdot | s_E, a_E), \\ \text{set } \tilde{g}^{(\mathbf{c}, \mathbf{u})}((\mathbf{c}_t, \mathbf{u}_t), \boldsymbol{\mu}_t) & \\ &= \begin{pmatrix} |\mathcal{S}||\mathcal{A}| \cdot 2\alpha (c_t(s, a) \mathbf{e}^{(s, a)} - \hat{c}(s, a) \mathbf{e}^{(s, a)}) + \mathbf{e}^{(s_E, a_E)} - \mathbf{e}^{(s_t, a_t)} \\ \frac{1}{(1-\gamma)} (\mathbf{e}^{s_t} - \gamma \mathbf{e}^{s'_t} - (\mathbf{e}^{s_E} - \gamma \mathbf{e}^{s'_E})) \end{pmatrix}. \end{aligned} \tag{1}$$

In Lemma 1, we show that this estimator is unbiased, and we provide a bound for its second moment.

Lemma 1. *Gradient estimator $\tilde{g}^{(\mathbf{c}, \mathbf{u})}((\mathbf{c}_t, \mathbf{u}_t), \boldsymbol{\mu}_t)$ is a $(v^{(\mathbf{c}, \mathbf{u})}, \|\cdot\|_2)$ -bounded estimator, with*

$$v^{(\mathbf{c}, \mathbf{u})} = 64\alpha^2 \cdot |\mathcal{S}||\mathcal{A}| + \frac{4(1 + \gamma^2)}{(1 - \gamma)^2} + 8.$$

For the $\boldsymbol{\mu}$ side, define the gradient estimator by

$$\begin{aligned} \text{sample } (s, a) &\sim \frac{1}{|\mathcal{S}||\mathcal{A}|}, s' \sim P(\cdot | s, a), \\ \text{set } \tilde{g}^\mu((\mathbf{c}_t, \mathbf{u}_t), \boldsymbol{\mu}_t) & \\ &= |\mathcal{S}||\mathcal{A}| \left(c_t(s, a) \mathbf{e}^{(s, a)} - \frac{1}{(1-\gamma)} (u_t(s) \mathbf{e}^{(s, a)} - \gamma u_t(s') \mathbf{e}^{(s, a)}) \right). \end{aligned} \tag{2}$$

As before, we will demonstrate unbiasedness and bound its second moment; however, this time we will also calculate a bound on its maximum entry.

Lemma 2. *Gradient estimator $\tilde{g}^\mu((\mathbf{c}_t, \mathbf{u}_t), \boldsymbol{\mu}_t)$ is a $(z^\mu, v^\mu, \|\cdot\|_{\Delta})$ -bounded estimator, with*

$$z^\mu = \frac{2|\mathcal{S}||\mathcal{A}|}{(1-\gamma)} \text{ and } v^\mu = |\mathcal{S}||\mathcal{A}| \left(2 + \frac{4(1 + \gamma^2)}{(1 - \gamma)^2} \right).$$

Using these gradient estimators and the bounds established above, we adapt the SMD algorithm originally designed for solving MDPs in Jin & Sidford (2020). Algorithm 1 presents the SMD method for (RLfD $_{\alpha}$). This algorithm iteratively computes bounded gradient estimators (Lines 3 and 5) by sampling from the occupancy measures and querying the oracle (Lines 2 and 4). The updates are then obtained using mirror descent steps followed by a projection (Lines 6 and 7). After T iterations, the algorithm returns the average of the iterates as an ϵ -approximate solution to (RLfD $_{\alpha}$).

Algorithm 1: Stochastic Mirror Descent for (RLfD $_{\alpha}$) (SMD-RLfD)

Parameters: Step-size $\eta^{(c,u)}$, η^{μ} , number of iterations T , accuracy level ϵ .

Input: State space \mathcal{S} , action space \mathcal{A} , transition oracle P , occupancy measure oracle μ_{π_E} , initial state distribution ν_0 , discount factor γ , initial $((c_0, u_0), \mu_0) \in \mathbb{B}_1^{|\mathcal{S}||\mathcal{A}|} \times \Delta^{|\mathcal{S}||\mathcal{A}|}$.

Output: An expected ϵ -approximate solution $((c^{\epsilon}, u^{\epsilon}), \mu^{\epsilon})$ for (RLfD $_{\alpha}$).

```

1 for  $t \leftarrow 0$  to  $T - 1$  do
  /*  $(c, u)$  gradient estimation */
2 Sample  $(s_t, a_t) \sim \mu_t$ ,  $s'_t \sim P(\cdot | s_t, a_t)$ ,  $(s_E, a_E) \sim \mu_{\pi_E}$ ,  $s'_E \sim P(\cdot | s_E, a_E)$ 
3 Compute:
      
$$\tilde{g}^{(c,u)}((c_t, u_t), \mu_t) = \left( \begin{array}{c} 2\alpha(c_t - \hat{c}) + \mu_{\pi_E} - \mu_t \\ \frac{1}{(1-\gamma)} (e^{s_t} - \gamma e^{s'_t} - (e^{s_E} - \gamma e^{s'_E})) \end{array} \right)$$

  /*  $\mu$  gradient estimation */
4 Sample  $(s, a) \sim \frac{1}{|\mathcal{S}||\mathcal{A}|}$ ,  $s' \sim P(\cdot | s, a)$ 
5 Compute:
      
$$\tilde{g}^{\mu}((c_t, u_t), \mu_t) = |\mathcal{S}||\mathcal{A}| \left( c_t(s, a)e^{(s,a)} - \frac{1}{(1-\gamma)} (u_t(s)e^{(s,a)} - \gamma u_t(s')e^{(s',a)}) \right)$$

  /* Mirror descent steps */
6  $(c_t, u_t) \leftarrow \Pi_{\mathbb{B}_1^{|\mathcal{S}||\mathcal{A}|} \times \mathbb{B}_1^{|\mathcal{S}|}}((c_{t-1}, u_{t-1}) - \eta^{(c,u)}\tilde{g}^{(c,u)}((c_{t-1}, u_{t-1}), \mu_{t-1}))$ 
7  $\mu_t \leftarrow \Pi_{\Delta^{|\mathcal{S}||\mathcal{A}|}}(\mu_{t-1} \circ \exp(-\eta^{\mu}\tilde{g}^{\mu}((c_{t-1}, u_{t-1}), \mu_{t-1})))$ 
8 return  $((c^{\epsilon}, u^{\epsilon}), \mu^{\epsilon}) \leftarrow \frac{1}{T} \sum_{t=1}^T ((c_t, u_t), \mu_t)$ 

```

Theorem 2. Given $\epsilon \in (0, 1)$, Algorithm 1 with step-size

$$\eta^{(c,u)} = \frac{\epsilon}{4v^{(c,u)}}, \quad \eta^{\mu} = \frac{\epsilon}{4v^{\mu}},$$

and gradient estimators defined in equations (1) and (2) finds an expected ϵ -approximate solution

$$\mathbb{E}[\text{Gap}((c^{\epsilon}, u^{\epsilon}), \mu^{\epsilon})] \leq \epsilon,$$

within any iteration number

$$T \geq \max \left\{ \mathcal{O} \left(\frac{\alpha^2 |\mathcal{S}|^3 |\mathcal{A}|^2}{\epsilon^2} \right), \mathcal{O} \left(\frac{|\mathcal{S}||\mathcal{A}| \log(|\mathcal{S}||\mathcal{A}|)}{\epsilon^2} \right) \right\}.$$

The number of iterations scales quadratically with the number of actions and cubically with the number of states. Theoretically, the number of iterations required depends on the parameter $\alpha \in \mathbb{R}_+$. When $\alpha = 0$, the number of iterations decreases significantly as the $|\mathcal{S}|^3$ and $|\mathcal{A}|^2$ terms vanish from the initial expression. This suggests that introducing the regularization $\alpha \|c - \hat{c}\|_2^2$ increases the complexity of the problem. Nevertheless, we will see in the next section that the regularization term helps to guide the search to uncover the true cost function.

Proposition 4. Let $((\mathbf{c}^\epsilon, \mathbf{u}^\epsilon), \boldsymbol{\mu}^\epsilon)$ be an expected ϵ -approximate solution for (RLfD_α) , where $\boldsymbol{\mu}^\epsilon$ induces a policy $\pi_{\boldsymbol{\mu}^\epsilon} \in \Pi_0$ defined by $\pi_{\boldsymbol{\mu}^\epsilon}(a|s) = \frac{\boldsymbol{\mu}^\epsilon(a,s)}{\sum_{a'} \boldsymbol{\mu}^\epsilon(s,a')}$. It then holds that

$$\mathbb{E} \left[\alpha \|\mathbf{c}^\epsilon - \hat{\mathbf{c}}\|_2^2 + \rho_{\mathbf{c}^\epsilon}(\pi_E) - \rho_{\mathbf{c}^\epsilon}(\pi_A) \right] \leq \epsilon + \alpha \|\mathbf{c}_A - \hat{\mathbf{c}}\|_2^2 + \rho_{\mathbf{c}_A}(\pi_E) - \rho_{\mathbf{c}_A}^*,$$

where $((\mathbf{c}_A, \mathbf{u}_A), \boldsymbol{\mu}_A)$ denotes the optimal solution for (RLfD_α) and π_A is the policy induced by $\boldsymbol{\mu}_A$.

Proof. As $((\mathbf{c}^\epsilon, \mathbf{u}^\epsilon), \boldsymbol{\mu}^\epsilon)$ is an ϵ -approximate solution we know that

$$\mathbb{E} \left[\mathcal{L}((\mathbf{c}^\epsilon, \mathbf{u}^\epsilon), \boldsymbol{\mu}_A) - \mathcal{L}((\mathbf{c}_A, \mathbf{V}_{\mathbf{c}_A}^{\pi_{\boldsymbol{\mu}^\epsilon}}), \boldsymbol{\mu}^\epsilon) \right] \leq \epsilon.$$

Moreover,

$$\begin{aligned} & \mathcal{L}((\mathbf{c}^\epsilon, \mathbf{u}^\epsilon), \boldsymbol{\mu}_A) - \mathcal{L}((\mathbf{c}_A, \mathbf{V}_{\mathbf{c}_A}^{\pi_{\boldsymbol{\mu}^\epsilon}}), \boldsymbol{\mu}^\epsilon) \\ &= \alpha \|\mathbf{c}^\epsilon - \hat{\mathbf{c}}\|_2^2 - \alpha \|\mathbf{c}_A - \hat{\mathbf{c}}\|_2^2 + \langle \boldsymbol{\mu}_{\pi_E} - \boldsymbol{\mu}_A, \mathbf{c}^\epsilon - \mathbf{T}_\gamma^\top \mathbf{u}^\epsilon \rangle - \langle \boldsymbol{\mu}_{\pi_E} - \boldsymbol{\mu}^\epsilon, \mathbf{c}_A - \mathbf{T}_\gamma^\top \mathbf{V}_{\mathbf{c}_A}^{\pi_{\boldsymbol{\mu}^\epsilon}} \rangle \\ &\stackrel{(i)}{=} \alpha \|\mathbf{c}^\epsilon - \hat{\mathbf{c}}\|_2^2 - \alpha \|\mathbf{c}_A - \hat{\mathbf{c}}\|_2^2 + \rho_{\mathbf{c}^\epsilon}(\pi_E) - \rho_{\mathbf{c}^\epsilon}(\pi_A) - \rho_{\mathbf{c}_A}(\pi_E) + \rho_{\mathbf{c}_A}(\pi_{\boldsymbol{\mu}^\epsilon}) \\ &\stackrel{(ii)}{\geq} \alpha \|\mathbf{c}^\epsilon - \hat{\mathbf{c}}\|_2^2 - \alpha \|\mathbf{c}_A - \hat{\mathbf{c}}\|_2^2 + \rho_{\mathbf{c}^\epsilon}(\pi_E) - \rho_{\mathbf{c}^\epsilon}(\pi_A) - \rho_{\mathbf{c}_A}(\pi_E) + \rho_{\mathbf{c}_A}(\pi_A), \end{aligned}$$

where (i) follows from $\langle \boldsymbol{\mu}_1 - \boldsymbol{\mu}_2, -\mathbf{T}_\gamma^\top \mathbf{u} \rangle = \langle \boldsymbol{\nu}_0, \mathbf{u} \rangle - \langle \boldsymbol{\nu}_0, \mathbf{u} \rangle = 0$ and Lemma 2 (Appendix B.1) in Kamoutsis et al. (2021) and (ii) from $\rho_{\mathbf{c}_A}^* = \rho_{\mathbf{c}_A}(\pi_A) \leq \rho_{\mathbf{c}_A}(\pi)$ for any policy $\pi \in \Pi_0$. Rearranging these terms, we arrive to

$$\mathbb{E} \left[\alpha \|\mathbf{c}^\epsilon - \hat{\mathbf{c}}\|_2^2 + \rho_{\mathbf{c}^\epsilon}(\pi_E) - \rho_{\mathbf{c}^\epsilon}(\pi_A) \right] \leq \epsilon + \alpha \|\mathbf{c}_A - \hat{\mathbf{c}}\|_2^2 + \rho_{\mathbf{c}_A}(\pi_E) - \rho_{\mathbf{c}_A}^*.$$

□

Proposition 4 establishes a connection between expected ϵ -approximate solutions for (RLfD_α) and its optimal solution. Specifically, it shows that an expected ϵ -approximate solution achieves an objective value that is at most ϵ worse than that of the optimal solution. Note that we do not assume that $\boldsymbol{\mu}^\epsilon$ is an occupancy measure, which is not always the case for an arbitrary $\boldsymbol{\mu} \in \Delta^{|S||A|}$.

5 Numerical experiments

We analyze the performance of the proposed framework using two case studies: a low-dimensional inventory management problem and a higher-dimensional Gridworld problem. The inventory example serves as a tractable system to build intuition and offer insights into the practical selection of proxy cost vector $\hat{\mathbf{c}}$. Moreover, we conduct ablation analyses on prior misspecification and expert suboptimality, and execute a direct comparison with the convex hull methodology of Kamoutsis et al. (2021). The Gridworld example is employed to demonstrate the method's convergence properties and quantify the specific impact of the regularization term on the learned cost vector in a higher-dimensional space.

To facilitate reproducibility, the complete source code and experimental setups are publicly available at <https://github.com/EstebanLeiva/apprenticeshiplearning.git>. Because SMD-RLfD yields expected ϵ -approximate solutions for (RLfD_α) , we account for stochasticity by executing the algorithm for N independent runs. Each run uses randomly generated initial vectors $((\mathbf{c}_0, \mathbf{u}_0), \boldsymbol{\mu}_0)$ and proceeds for T iterations; we report the average of the resulting outputs.

5.1 Single-product inventory control

The single-product stochastic inventory control problem is a classic model for finite state MDPs (Puterman, 1994). It is defined by a state space $\mathcal{S} = \{0, 1, \dots, M\}$ representing the inventory level on hand, and an action space $\mathcal{A}(s) = \{0, 1, \dots, M - s\}$ representing the quantity ordered, where $M = 15$ is the maximum capacity. The system transition from the inventory level $L = s + a$ to the next state $s' = \max(0, L - D)$

is governed by a stochastic demand D , which is modeled using a known Poisson distribution with mean $\lambda = 10$. The goal is to minimize the expected operational cost $c(s, a)$, which is linear with respect to order cost $c_o = 3$, holding cost $c_h = 0.5$, and sell price $c_s = 15$. This cost is defined by the equation $c(s, a) = c_o \cdot a + c_h \cdot (s + a) - c_s \cdot \mathbb{E}[\min(s + a, D)]$, where $\mathbb{E}[\min(s + a, D)]$ is the expected number of units sold. Note that the dimension of the cost vector depends on M , but it is completely determined by the three parameters above. At each timestep, the expert observes the inventory level s and selects an order quantity a (assuming instantaneous replenishment), after which demand d is fulfilled with no backlog, and the system updates the inventory level for the next iteration. Finally, the discount factor is fixed to 0.9, and initial states are chosen uniformly.

Solving (MDP- P_c) to optimality yields a policy that consistently restocks to a level of 14 units (Figure 3). The policy avoids utilizing the full capacity, which can be understood as a consequence of the relationship between holding costs and expected demand. We begin with a single instance of our framework. Consider a suboptimal

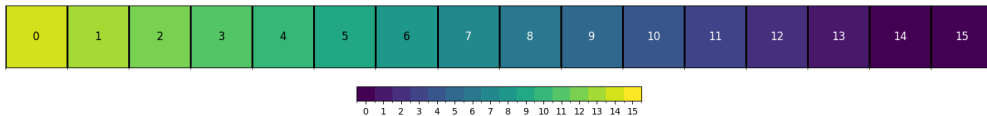


Figure 3: Visualization of the optimal policy. Each cell represents a state, with the inventory level displayed in the center. The color coding indicates the optimal order quantity for that state. For example, at an inventory level of $s=1$, the optimal action is to order 13 units.

expert whose policy is optimal with respect to a misspecified cost function parameterized by $c_o = 5$, $c_h = 8$, and $c_s = 15$. Intuitively, because this expert perceives a significantly higher holding cost, the resulting policy maintains a reduced inventory level (Figure 4). Having defined the suboptimal expert, we next require a

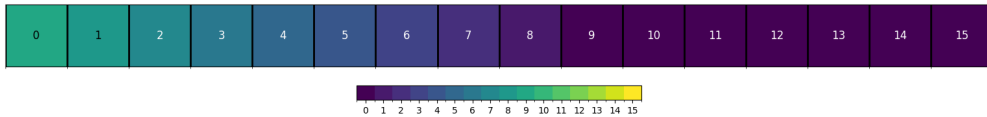


Figure 4: Visualization of the suboptimal policy.

proxy cost vector \hat{c} representing our prior beliefs on the cost vector. Crucially, this prior must be established “independently” of the observed expert to avoid circularity. In this context, independence implies that \hat{c} is derived exclusively from exogenous information, such as market prices or physical constraints, rather than being inferred from the expert’s trajectories. If \hat{c} were derived exclusively from the observed demonstrations, it would fall within the inverse optimality set $\Theta^{\text{inv}}(\mu_{\pi_E})$, thereby eliminating the necessary trade-off between the expert and the prior (as illustrated in Figure 2). Therefore, based strictly on the problem structure and excluding expert data, we suppose \hat{c} is defined using the parameters $(c_o, c_h, c_s)=(4,2,14)$. We set $\alpha = 0.1$

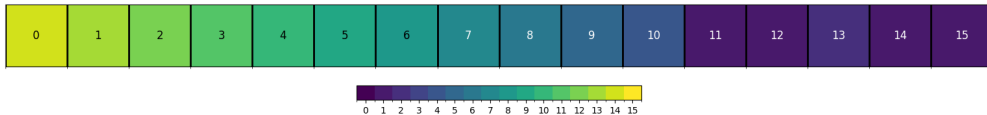
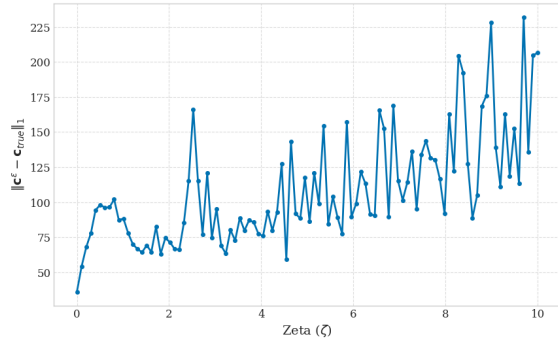


Figure 5: Visualization of the apprentice policy.

and execute the SMD algorithm for $N = 10^3$ independent runs, with $T = 10^4$ iterations and both step-sizes fixed at 10^{-2} . Figure 5 illustrates the policy induced by μ^ϵ . As observed, the learned policy is identical to the optimal policy with the exception of the last five inventory states, where it orders between one and two units. This demonstrates that the method is capable of recovering a near-optimal policy. To recover the scalar parameters (c_o, c_h, c_s) from the high-dimensional learned cost vector \mathbf{c}_A , we solve a linear least-squares regression problem of the form $\min_{\mathbf{x}} \|\mathbf{A}\mathbf{x} - \mathbf{c}_A\|_2^2$. Here, $\mathbf{x} = [c_o, c_h, c_s]^\top$, and the row of the design matrix \mathbf{A}



(a) Recovered cost vectors.



(b) ℓ_1 distance between the learned cost vector and the truth.

Figure 6: Effect of perturbations in the proxy cost vector $\hat{\mathbf{c}}$ on the learned cost.

corresponding to a state-action pair (s, a) is defined by the feature vector $\mathbf{A}_{(s,a)} = [a, s+a, -\mathbb{E}[\min(s+a, D)]]$. Solving this regression, we obtain the recovered parameters $(c_o, c_h, c_s) = (3.4, 2.3, 14.1)$. The following sections discuss the effect of the choice of $\hat{\mathbf{c}}$ and the suboptimality of the expert in more detail.

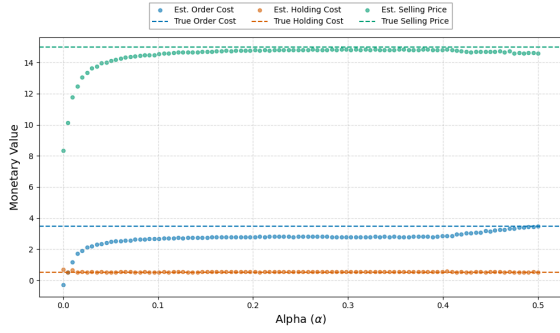
5.1.1 Misspecified prior beliefs

We assess the sensitivity of our framework to misspecifications in the proxy cost vector $\hat{\mathbf{c}}$. To quantify this, we consider the single-product inventory problem with true parameters $(c_o, c_h, c_s) = (3, 0.5, 15)$. We fix the inputs to the problem (RLfD $_{\alpha}$) as follows: we use an optimal expert (see Figure 3) and set the regularization parameter $\alpha = 0.1$. With these inputs held constant, we perturb the proxy cost vector to analyze the effect of deviations from the ground truth. We introduce noise to the proxy by defining $\hat{c}_o = 3 + \zeta(0.3u_1)$, $\hat{c}_h = 0.5 + \zeta(0.05u_2)$, and $\hat{c}_s = 15 + \zeta(1.5u_3)$, where $u_i \sim U[-1, 1]$ are i.i.d. random variables. This formulation scales the perturbation such that $\zeta = 1$ corresponds to a maximum deviation of 10% per coordinate. We evaluate this sensitivity across a grid of 100 equally spaced values for $\zeta \in [0, 10]$, representing error magnitudes ranging from 0% to 100%. For each ζ , we generate 5 independent realizations of the random noise, run the SMD algorithm, and report the average of the recovered costs and the average ℓ_1 distance between the learned cost vector \mathbf{c}^{ϵ} and the true cost vector \mathbf{c}_{true} . Figure 6(a) shows the difference between the recovered parameters that define the cost vector and the true parameters, while Figure 6(b) shows the ℓ_1 -norm between the actual cost vectors. Note that priority is given to the highest cost (selling price), and the distance increases with ζ as expected. Let us remark that SMD-RLfD is an approximate algorithm; hence, the differences are never null.

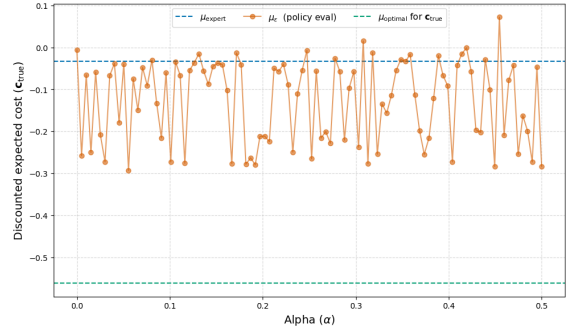
5.1.2 Expert suboptimality and regularization

Our framework is designed to mitigate potential expert suboptimality by regularizing the solution against a prior belief. Our objective is to demonstrate that if the expert is suboptimal, a correctly specified prior can “help” the learning process and recover a performant cost vector and policy. To quantify this impact, we revisit the inventory problem defined by $(c_o, c_h, c_s) = (3, 0.5, 15)$. We establish a controlled setting by fixing a suboptimal expert given by Figure 4 and providing the true cost vector as the proxy $\hat{\mathbf{c}}$. We then vary the regularization strength α across the interval $[0, 0.5]$ and evaluate the learned cost vector, see Figure 7(a), and the resulting apprentice policy’s performance against the true cost vector, see Figure 7(b). As anticipated, the use of an informative proxy cost vector $\hat{\mathbf{c}}$ facilitates the recovery of the true cost vector as the regularization parameter α increases. Moreover, the policy induced by the learned μ^{ϵ} achieves a consistently lower discounted expected cost with respect to the true cost vector \mathbf{c}_{true} across the tested values of α . This indicates that the learned policy is robust to variations in α and outperforms the expert. Note that the discounted expected cost for the policy induced by $\pi_{\mu^{\epsilon}}$ was computed using policy evaluation.

Using the same experimental setting, we analyze the quantity $\alpha\|\hat{\mathbf{c}} - \mathbf{c}^{\epsilon}\| + \rho_{\mathbf{c}^{\epsilon}}(\pi_E) - \rho_{\mathbf{c}^{\epsilon}}(\pi_A)$. As established in Proposition 4, this expression links the outputs of SMD-RLfD to the optimal values of IO-AL $_{\alpha}$, which are



(a) Recovered cost vectors.



(b) Discounted expected cost.

Figure 7: Learned cost vectors and apprentice policies under varying regularization levels α .

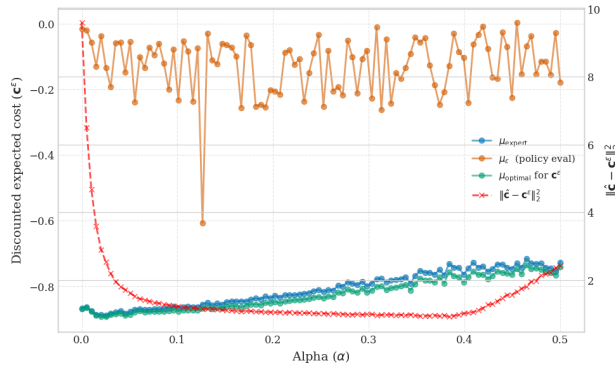


Figure 8: Illustration of Propositions 3 and 4.

characterized in Proposition 3. Figure 8 illustrates the trade-off given by the proposition. The left vertical axis displays the discounted expected cost with respect to the learned cost vector \mathbf{c}^ϵ for three policies: the expert policy μ_E , the policy induced by μ^ϵ , and the optimal policy for \mathbf{c}^ϵ . The right vertical axis plots the norm of the difference $\|\hat{\mathbf{c}} - \mathbf{c}^\epsilon\|$ across varying values of α .

We observe a clear balance between these terms: as α increases, the optimization places greater weight on the norm, reducing $\|\hat{\mathbf{c}} - \mathbf{c}^\epsilon\|$ while allowing the performance gap $\rho_{\mathbf{c}^\epsilon}(\pi_E) - \rho_{\mathbf{c}^\epsilon}(\pi_A)$ to widen. Conversely, when α is small, the performance gap becomes negligible, while the norm difference increases inversely. In any case, note that \mathbf{c}^ϵ is chosen such that the expert policy is nearly optimal. Finally, we observe that the discounted expected cost of the policy induced by μ^ϵ remains stable to variations in α .

5.1.3 Restricting the search space to a convex hull

As it was noted in Section 3.2, the apprenticeship learning literature typically assumes that the true cost vector \mathbf{c}_{true} lies within the convex hull of a prespecified set of basis vectors $\{\mathbf{c}_i\}_{i=1}^{n_c}$ (Syed et al., 2008; Kamoutsi et al., 2021). While this assumption reduces the dimensionality of the search space from $|\mathcal{S}||\mathcal{A}|$ to n_c , it limits flexibility and requires a robust method for feature engineering. Since the algorithm presented in Kamoutsi et al. (2021) targets a linearly relaxed saddle-point formulation with different convergence properties, we adapt SMD-RLfD to optimize over the vectors $\mathbf{c}_w = \mathbf{C}\mathbf{w}$, where $\mathbf{w} \in \Delta^{n_c}$ and the columns of $\mathbf{C} \in \mathbb{R}^{|\mathcal{S}||\mathcal{A}| \times n_c}$ correspond to the basis vectors. This adaptation entails updating the gradient estimators for the objective function (RLfD $_\alpha$) and shifting the mirror descent step from the box $\mathbb{B}_1^{|\mathcal{S}||\mathcal{A}|}$ to the simplex Δ^{n_c} . Moreover, setting $\alpha = 0$ in this adapted formulation recovers the problem solved by Kamoutsi et al. (2021), as guaranteed by the equality in Theorem 1. This enables a controlled comparison of the optimization domains by applying both the original and modified algorithms to the equivalent unregularized problem where $\alpha = 0$.

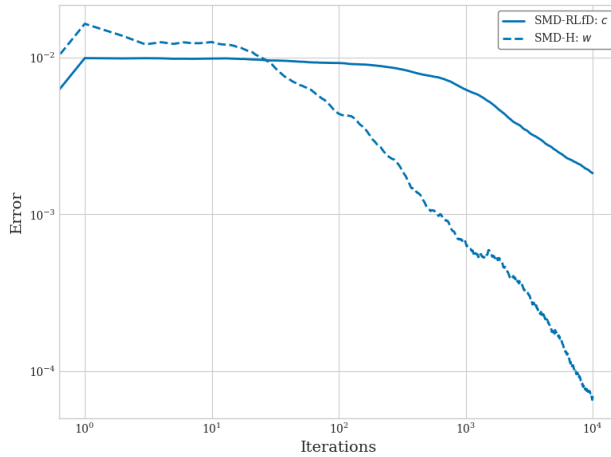


Figure 9: Impact of the search space geometry (convex hull vs. box) on the convergence rate of the cost vector.

The inventory problem serves as an ideal testbed for the convex hull formulation because its cost vector is a linear combination of three features: ordering \mathbf{c}^o , holding \mathbf{c}^h , and sales \mathbf{c}^s . This structure effectively reduces the dimensionality of the cost parameters from $|\mathcal{S}||\mathcal{A}|$ to 3. We compare the convergence of SMD-RLfD against the modified variant (SMD-H) that optimizes weights $\mathbf{w} \in \Delta^3$, when considering an optimal expert and maintaining common algorithm parameters $T = 10,000$ and $N = 100$. Figure 9 displays the ℓ_1 -norm of the difference between solutions at consecutive iterations. The results indicate that the convex hull approach accelerates the convergence of \mathbf{w} , a behavior consistent with the suitability of mirror descent for optimization over a simplex domain.

We extend the experimental evaluation to varying state space dimensions. For each configuration, we consider an optimal expert policy using the fixed parameters $(c_o, c_h, c_s) = (3, 0.5, 15)$. Figure 10 presents the discounted expected cost of the resulting apprentice policies with respect to the true cost vector. We observe that while the convex hull formulation yields similar performance in smaller state spaces, our framework outperforms it as the problem dimension grows. This trend may be attributed to the stochastic nature of the solution algorithms. The box formulation exhibits greater flexibility in adapting to error variations, whereas the convex hull proves too rigid to adapt effectively in higher dimensions.

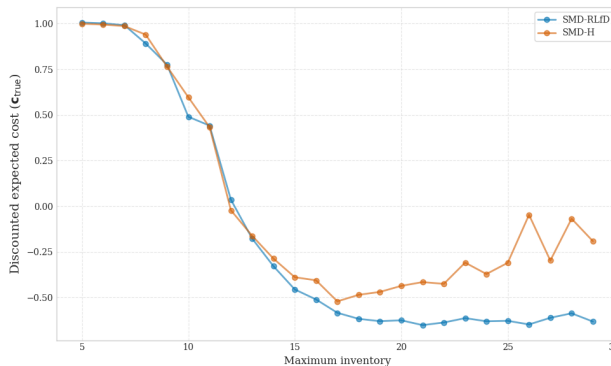


Figure 10: Comparison of the discounted expected cost between the proposed framework and the convex hull approach across state space sizes.

5.2 Gridworld

We use a standard $H \times W$ Gridworld environment (Figure 11(a)), where each cell is a unique state. Obstacles (shown in red) incur a cost of 1, terminal cells (shown in green) incur a cost of -1 , and all other cells (shown in white) incur a cost of 0. The action set is $\{\text{up, down, left, right}\}$, but a “wind” introduces a 20% chance of drifting left or otherwise altering the intended move. If the resulting move is out of bounds, the agent remains in the same cell. The discount factor is 0.7, and initial states are chosen uniformly. We solve the corresponding (MDP- \mathcal{P}_c) with a linear solver to obtain the optimal occupancy measure (Figure 11(b)). To construct a suboptimal expert, we terminate the solver early and use the resulting μ as the expert’s occupancy measure (Figure 11(c)). To visualize the policies induced by these occupancy measures, we extract the most likely action at each state by computing $\arg \max_{a \in \mathcal{A}} \mu(s, a)$ and display it in the corresponding cell. Unlike

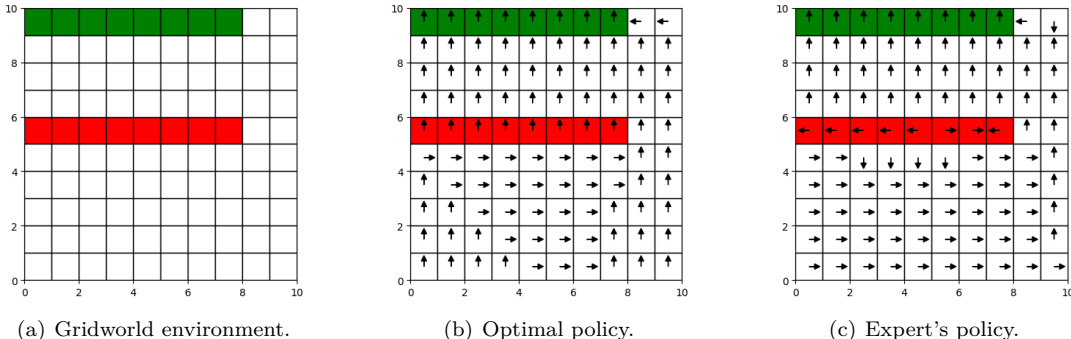


Figure 11: Illustration of the Gridworld environment, the optimal policy, and the expert’s policy.

the inventory control example, defining the cost vector in this setting as a convex combination of basis vectors is not straightforward. This highlights a key advantage of our framework’s flexibility: it obviates the need for preliminary feature engineering or basis estimation processes that are often time-consuming and prone to error. Consequently, our method is directly applicable without requiring these preprocessing steps, since even without a prior belief of the cost vector, we can just set $\alpha = 0$. Furthermore, modeling this region as a convex hull would require $2^{|\mathcal{S}||\mathcal{A}|}$ basis vectors, rendering the approach computationally intractable, even for small state-action spaces.

5.2.1 Impact of regularization on the learned cost vector

We study the effect of the regularization term $\alpha \|\mathbf{c} - \hat{\mathbf{c}}\|_2^2$ on problem (RLfD $_\alpha$) to demonstrate that incorporating prior knowledge, even when imperfect, yields learned cost vectors that align more closely with the true environment. To this end, we define a cost vector $\hat{\mathbf{c}}$ that is zero everywhere except for a randomly selected subset of obstacle and goal states. This choice was made based on practical considerations, as in most real-world scenarios, we rarely have access to a highly accurate estimate of the cost vector. Specifically, for obstacles, $\hat{\mathbf{c}}$ is set to 1 for a randomly selected 50% of the obstacle states, while for goal states, $\hat{\mathbf{c}}$ is set to -1 for a randomly chosen 50% of them. Moreover, regarding the algorithm’s parameters, we chose $N = 20$, $T = 10^5$, and both step-sizes as 10^{-2} .

Figure 12 depicts the learned cost vectors for each action $\{\text{up, down, left, right}\}$ under varying levels of regularization α . As α increases, the cost vectors display more white regions, indicating near-zero cost values, and more accurately highlight the main obstacles. In turn, this leads to a better approximation of the true cost structure. However, when the regularization is too strong, it may overly penalize costs associated with obstacle areas that are less frequently demonstrated, thereby ignoring parts of the environment that do not appear in the demonstration data. Consequently, selecting an appropriate α is crucial to achieve a cost vector that balances fidelity to the true environment and robustness in identifying cost structures that are not present in the estimate $\hat{\mathbf{c}}$.

Figure 13 displays the apprentice policy obtained using SMD-RLfD for various values of α . Notably, when α is set to 0.005 or 0.001, the apprentice policy closely resembles the one derived by exclusively weighting

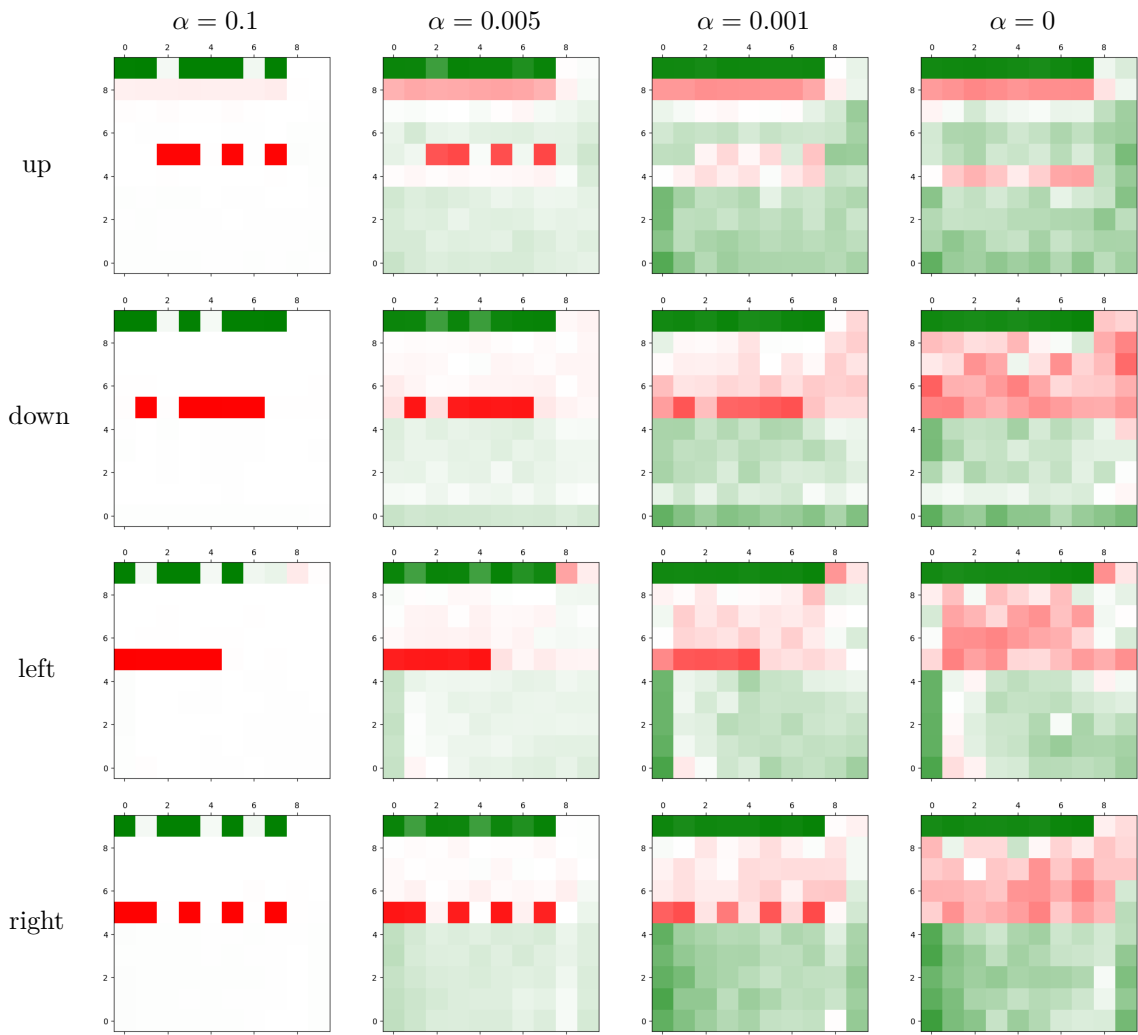


Figure 12: Effect of the regularization on the cost vector.

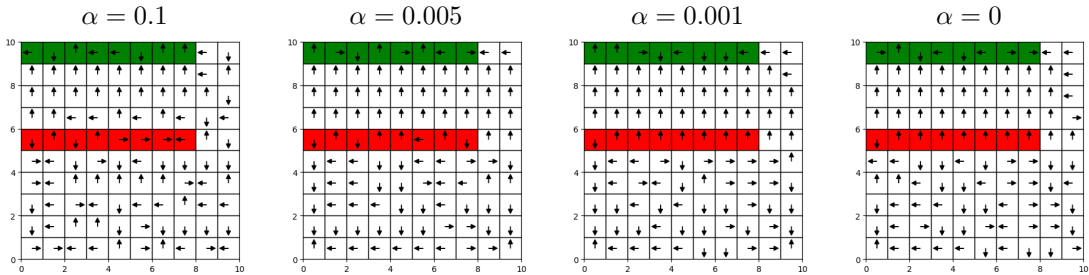


Figure 13: Effect of regularization on the apprentice policy.

the expert’s policy (i.e., $\alpha = 0$). This observation is significant, as the previous analysis demonstrated that incorporating regularization yields a cost vector for the apprentice policies that aligns more closely with the true cost vector.

5.2.2 Convergence and regularization

In the same experimental setting, we examined the convergence of the solutions up to iteration $t < T$ by computing the ℓ_1 -norm of the difference between the solutions at iterations t and $t - 1$. We plotted this norm for each of the α values considered in the previous experiments. According to this sense of convergence, all α values exhibit comparable convergence rates for \mathbf{u} and $\boldsymbol{\mu}$. However, for \mathbf{c} , the convergence rate at $\alpha = 0.1$ is faster than that observed for smaller values of α . This behavior aligns with the increased penalty imposed for deviating from $\hat{\mathbf{c}}$ under stronger regularization, thereby accelerating convergence for \mathbf{c} .

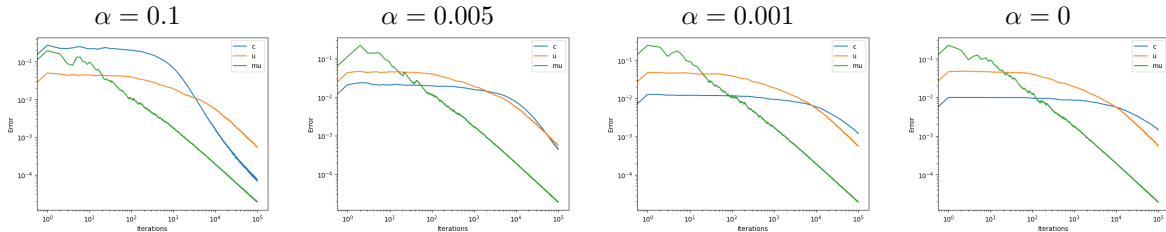


Figure 14: Effect of regularization on the difference of solutions found between iterations.

However, it is important to note that Theorem 2 characterizes convergence in terms of the duality gap. In Figure 15, we compute the duality gap of the solution every 25 iterations, using IPOPT (Wächter & Biegler, 2006). The algorithm parameters remain unchanged, except that, due to computational constraints, we reduce the grid size to 6×6 and limit the execution to $T = 10^4$ iterations. As expected from the results of Theorem 2, stronger regularization leads to slower convergence of the duality gap, a trend illustrated in this figure. While we did not use the theoretically prescribed step sizes due to their small magnitude, the figure still offers valuable insights into how regularization affects the convergence behavior.

6 Conclusion

This work establishes a unified perspective on IRL and AL by grounding them in the IO framework for MDPs. A key theoretical contribution is the demonstration that the convex-analytic AL formalism proposed by Kamoutsi et al. (2021) emerges as a specific relaxation of this broader framework. Central to the proposed methodology is the incorporation of prior beliefs on the cost function to address the inherent ill-posedness of the IRL problem, where multiple cost functions can explain the same expert behavior. By introducing a proxy cost vector $\hat{\mathbf{c}}$ and a regularization parameter α , we formulate the (IO-AL) $_{\alpha}$ problem tailored for the scenarios in which the expert is suboptimal. This approach is designed to mitigate the impact of expert suboptimality, with the regularization term serving as a mechanism to modulate the trade-off between fidelity to the observed demonstrations and adherence to the informative prior.

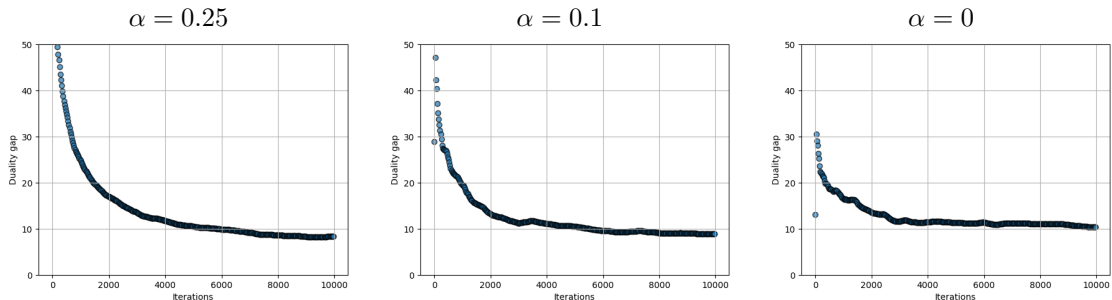


Figure 15: Duality gap convergence.

To solve the optimization problem posed in (IO-AL_α) , we leverage Lagrangian duality to recast the formulation as a convex-concave-min-max problem suitable for stochastic mirror descent methods. We introduce the SMD-RLfD algorithm, an adaptation of the method proposed by Jin & Sidford (2020) to solve MDPs, and derive the necessary gradient estimators for this framework. Furthermore, we establish convergence guarantees, explicitly characterizing the relationship between the expected ϵ -approximate solutions generated by SMD-RLfD and the optimal solution of the original formulation (IO-AL_α) .

Numerical experiments underscore the critical role of regularization on learning performance. Our ablation analysis reveals that in scenarios involving a suboptimal expert and an informative proxy, increasing the regularization parameter α significantly improves the alignment between the recovered cost vectors and the ground truth. The resulting induced policy is notably robust to variations in α and consistently outperforms the expert. In comparison to the convex hull approach of Kamoutsi et al. (2021), we find that while the simplex-based formulation may offer faster convergence, our framework yields induced policies with superior performance as the state space expands. Furthermore, experiments on higher-dimensional Gridworld environments highlight the importance of regularization in learning a cost vector that correctly approximates the true cost vector and corroborate that stronger regularization accelerates the convergence of the cost vector; however, consistent with Theorem 2, this comes at the expense of slower convergence for the duality gap.

Future research could extend our methodology in several meaningful directions. First, establishing a criterion for selecting the regularization parameter α remains an open challenge. Second, in scenarios where the cost vector is known to be sparse (see the Gridworld example in Section 5.2), it would be useful to analyze the problem (IO-AL_α) with the ℓ_0 norm in the objective, $\|\mathbf{c}\|_0$, to explicitly enforce sparsity. Finally, further work is warranted to assess the scalability of this method to large-scale, high-dimensional problems and to develop robust techniques for constructing the proxy cost vector in complex real-world scenarios.

Acknowledgements

We thank Mateo Campo for his helpful insights. M. Junca was supported by the Research Fund of Facultad de Ciencias, Universidad de Los Andes INV-2025-213-3470.

References

- Pieter Abbeel and Andrew Y. Ng. Apprenticeship learning via inverse reinforcement learning. In *Proceedings of the Twenty-First International Conference on Machine Learning, ICML '04*, pp. 1, New York, NY, USA, 2004. Association for Computing Machinery. ISBN 1581138385. doi: 10.1145/1015330.1015430. URL <https://doi.org/10.1145/1015330.1015430>.
- Dario Amodei, Chris Olah, Jacob Steinhardt, Paul Christiano, John Schulman, and Dan Mané. Concrete problems in ai safety, 2016. URL <https://arxiv.org/abs/1606.06565>.
- Dimitris Bertsimas and John Tsitsiklis. *Introduction to Linear Optimization*. Athena Scientific, 1st edition, 1997. ISBN 1886529191.

-
- Daniel Brown, Wonjoon Goo, Prabhat Nagarajan, and Scott Niekum. Extrapolating beyond suboptimal demonstrations via inverse reinforcement learning from observations. In Kamalika Chaudhuri and Ruslan Salakhutdinov (eds.), *Proceedings of the 36th International Conference on Machine Learning*, volume 97 of *Proceedings of Machine Learning Research*, pp. 783–792. PMLR, 09–15 Jun 2019. URL <https://proceedings.mlr.press/v97/brown19a.html>.
- Yair Carmon, Yujia Jin, Aaron Sidford, and Kevin Tian. Variance reduction for matrix games. In H. Wallach, H. Larochelle, A. Beygelzimer, F. d'Alché-Buc, E. Fox, and R. Garnett (eds.), *Advances in Neural Information Processing Systems*, volume 32. Curran Associates, Inc., 2019. URL https://proceedings.neurips.cc/paper_files/paper/2019/file/6c442e0e996fa84f344a14927703a8c1-Paper.pdf.
- Timothy C. Y. Chan, Rafid Mahmood, and Ian Yihang Zhu. Inverse optimization: Theory and applications. *Operations Research*, 0(0):null, 2023. doi: 10.1287/opre.2022.0382. URL <https://doi.org/10.1287/opre.2022.0382>.
- Letian Chen, Rohan Paleja, and Matthew Gombolay. Learning from suboptimal demonstration via self-supervised reward regression. In *Conference on robot learning*, pp. 1262–1277. PMLR, 2021.
- Zeynep Erkin, Matthew D. Bailey, Lisa M. Maillart, Andrew J. Schaefer, and Mark S. Roberts. Eliciting Patients’ Revealed Preferences: An Inverse Markov Decision Process Approach. *Decision Analysis*, 7(4): 358–365, December 2010. doi: 10.1287/deca.1100.0185. URL <https://ideas.repec.org/a/inm/ordeca/v7y2010i4p358-365.html>.
- Dylan Hadfield-Menell, Smitha Milli, Pieter Abbeel, Stuart Russell, and Anca Dragan. Inverse reward design, 2020. URL <https://arxiv.org/abs/1711.02827>.
- Jonathan Ho and Stefano Ermon. Generative adversarial imitation learning. In D. Lee, M. Sugiyama, U. Luxburg, I. Guyon, and R. Garnett (eds.), *Advances in Neural Information Processing Systems*, volume 29. Curran Associates, Inc., 2016. URL https://proceedings.neurips.cc/paper_files/paper/2016/file/cc7e2b878868cbae992d1fb743995d8f-Paper.pdf.
- Yujia Jin and Aaron Sidford. Efficiently solving mdps with stochastic mirror descent. *CoRR*, abs/2008.12776, 2020. URL <https://arxiv.org/abs/2008.12776>.
- Angeliki Kamoutsi, Goran Banjac, and John Lygeros. Efficient performance bounds for primal-dual reinforcement learning from demonstrations. *CoRR*, abs/2112.14004, 2021. URL <https://arxiv.org/abs/2112.14004>.
- Filippo Lazzati, Mirco Mutti, and Alberto Metelli. Reward compatibility: A framework for inverse rl, 2025. URL <https://arxiv.org/abs/2501.07996>.
- David Lindner, Andreas Krause, and Giorgia Ramponi. Active exploration for inverse reinforcement learning. In *Proceedings of the 36th International Conference on Neural Information Processing Systems, NIPS ’22*, Red Hook, NY, USA, 2022. Curran Associates Inc. ISBN 9781713871088.
- Alberto Maria Metelli, Giorgia Ramponi, Alessandro Concetti, and Marcello Restelli. Provably efficient learning of transferable rewards. In Marina Meila and Tong Zhang (eds.), *Proceedings of the 38th International Conference on Machine Learning*, volume 139 of *Proceedings of Machine Learning Research*, pp. 7665–7676. PMLR, 18–24 Jul 2021. URL <https://proceedings.mlr.press/v139/metelli21a.html>.
- Alberto Maria Metelli, Filippo Lazzati, and Marcello Restelli. Towards theoretical understanding of inverse reinforcement learning. In *Proceedings of the 40th International Conference on Machine Learning, ICML’23*. JMLR.org, 2023.
- Andrew Y. Ng and Stuart J. Russell. Algorithms for inverse reinforcement learning. In *Proceedings of the Seventeenth International Conference on Machine Learning, ICML ’00*, pp. 663–670, San Francisco, CA, USA, 2000. Morgan Kaufmann Publishers Inc. ISBN 1558607072.

-
- Martin L. Puterman. *Markov Decision Processes: Discrete Stochastic Dynamic Programming*. John Wiley & Sons, Inc., USA, 1st edition, 1994. ISBN 0471619779.
- Deepak Ramachandran and Eyal Amir. Bayesian inverse reinforcement learning. In *Proceedings of the 20th International Joint Conference on Artificial Intelligence, IJCAI'07*, pp. 2586–2591, San Francisco, CA, USA, 2007. Morgan Kaufmann Publishers Inc.
- Nathan D. Ratliff, J. Andrew Bagnell, and Martin A. Zinkevich. Maximum margin planning. In *Proceedings of the 23rd International Conference on Machine Learning, ICML '06*, pp. 729–736, New York, NY, USA, 2006. Association for Computing Machinery. ISBN 1595933832. doi: 10.1145/1143844.1143936. URL <https://doi.org/10.1145/1143844.1143936>.
- Stuart Russell. Learning agents for uncertain environments (extended abstract). In *Proceedings of the Eleventh Annual Conference on Computational Learning Theory, COLT' 98*, pp. 101–103, New York, NY, USA, 1998. Association for Computing Machinery. ISBN 1581130570. doi: 10.1145/279943.279964. URL <https://doi.org/10.1145/279943.279964>.
- Umar Syed and Robert E Schapire. A game-theoretic approach to apprenticeship learning. In J. Platt, D. Koller, Y. Singer, and S. Roweis (eds.), *Advances in Neural Information Processing Systems*, volume 20. Curran Associates, Inc., 2007. URL https://proceedings.neurips.cc/paper_files/paper/2007/file/ca3ec598002d2e7662e2ef4bdd58278b-Paper.pdf.
- Umar Syed, Michael Bowling, and Robert E. Schapire. Apprenticeship learning using linear programming. In *Proceedings of the 25th International Conference on Machine Learning, ICML '08*, pp. 1032–1039, New York, NY, USA, 2008. Association for Computing Machinery. ISBN 9781605582054. doi: 10.1145/1390156.1390286. URL <https://doi.org/10.1145/1390156.1390286>.
- Andreas Wächter and Lorenz T. Biegler. On the implementation of an interior-point filter line-search algorithm for large-scale nonlinear programming. *Math. Program.*, 106(1):25–57, March 2006. ISSN 0025-5610.
- Yunke Wang, Chang Xu, Bo Du, and Honglak Lee. Learning to weight imperfect demonstrations. In *International Conference on Machine Learning*, pp. 10961–10970. PMLR, 2021.
- Brian D. Ziebart, Andrew Maas, J. Andrew Bagnell, and Anind K. Dey. Maximum entropy inverse reinforcement learning. In *Proceedings of the 23rd National Conference on Artificial Intelligence - Volume 3, AAAI'08*, pp. 1433–1438. AAAI Press, 2008. ISBN 9781577353683.

A Appendix - Some proofs

A.1 MDPs

Lemma 3. *Given a MDP with discount factor $\gamma \in (0, 1)$, then the value function satisfies*

$$V_{\mathbf{c}}^{\pi}(s) \leq \|\mathbf{c}\|_{\infty} = 1$$

for any policy $\pi \in \Pi_0$ and any state $s \in \mathcal{S}$.

Proof. Given a policy $\pi \in \Pi_0$ and a state $s \in \mathcal{S}$ the value function

$$\begin{aligned} V_{\mathbf{c}}^{\pi}(s) &= (1 - \gamma) \mathbb{E}_s^{\pi} \left[\sum_{t=0}^{\infty} \gamma^t c(s_t, a_t) \right] \\ &\leq (1 - \gamma) \mathbb{E}_s^{\pi} \left[\sum_{t=0}^{\infty} \gamma^t \|\mathbf{c}\|_{\infty} \right] \\ &= (1 - \gamma) \frac{1}{(1 - \gamma)} \|\mathbf{c}\|_{\infty} \\ &= 1. \end{aligned}$$

□

A.2 Gradient estimation

Proof of Lemma 1. The unbiasedness follows from the following observations

$$\begin{aligned} & \sum_{s,a} \frac{|\mathcal{S}||\mathcal{A}|}{|\mathcal{S}||\mathcal{A}|} \cdot 2\alpha \left(c_t(s,a) \mathbf{e}^{(s,a)} - \hat{c}(s,a) \mathbf{e}^{(s,a)} \right) \\ & + \sum_{s_E, a_E} \mu_{\pi_E}(s_E, a_E) \mathbf{e}^{(s_E, a_E)} - \sum_{s_t, a_t} \mu_t(s_t, a_t) \mathbf{e}^{(s_t, a_t)} \\ & = 2\alpha(\mathbf{c}_t - \hat{\mathbf{c}}) + \boldsymbol{\mu}_{\pi_E} - \boldsymbol{\mu}_t \end{aligned}$$

and

$$\begin{aligned} & \frac{1}{(1-\gamma)} \sum_{s'_t, a_t, s_t} \mu_t(s_t, a_t) P(s'_t | s_t, a_t) (\mathbf{e}^{(s_t)} - \gamma \mathbf{e}^{(s'_t)}) \\ & = \frac{1}{(1-\gamma)} \left(\sum_{s_t, a_t} \mu_t(s_t, a_t) \mathbf{e}^{(s_t)} - \gamma \sum_{s'_t, a_t, s_t} \mu_t(s_t, a_t) P(s'_t | s_t, a_t) \mathbf{e}^{(s'_t)} \right) \\ & = \frac{1}{(1-\gamma)} (\mathbf{B}\boldsymbol{\mu} - \gamma \mathbf{P}\boldsymbol{\mu}) \\ & = \mathbf{T}_\gamma \boldsymbol{\mu}. \end{aligned}$$

Thus, we obtain

$$\mathbb{E} \left[\tilde{g}^{(c, \mathbf{u})}((\mathbf{c}, \mathbf{u}), \boldsymbol{\mu}) \right] = \begin{pmatrix} 2\alpha(\mathbf{c}_t - \hat{\mathbf{c}}) + \boldsymbol{\mu}_{\pi_E} - \boldsymbol{\mu}_t \\ \mathbf{T}_\gamma \boldsymbol{\mu} - \mathbf{T}_\gamma \boldsymbol{\mu}_{\pi_E} \end{pmatrix}.$$

To prove the bound on the second-moment, note that

$$\begin{aligned} & \mathbb{E} \left[\left\| |\mathcal{S}||\mathcal{A}| \cdot 2\alpha \left(c_t(s,a) \mathbf{e}^{(s,a)} - \hat{c}(s,a) \mathbf{e}^{(s,a)} \right) + \mathbf{e}^{(s_E, a_E)} - \mathbf{e}^{(s_t, a_t)} \right\|_2^2 \right] \\ & \leq 2\mathbb{E} \left[4|\mathcal{S}||\mathcal{A}|\alpha^2 \left\| c_t(s,a) \mathbf{e}^{(s,a)} - \hat{c}(s,a) \mathbf{e}^{(s,a)} \right\|_2^2 + \left\| \mathbf{e}^{(s_E, a_E)} - \mathbf{e}^{(s_t, a_t)} \right\|_2^2 \right] \\ & \leq 2\mathbb{E} [4|\mathcal{S}||\mathcal{A}|\alpha^2 \cdot 4 + 2] \\ & = 32|\mathcal{S}||\mathcal{A}|\alpha^2 + 4, \end{aligned}$$

and

$$\begin{aligned} \mathbb{E} \left[\left\| \frac{1}{(1-\gamma)} \left(\mathbf{e}^{(s_t)} - \gamma \mathbf{e}^{(s'_t)} - (\mathbf{e}^{(s_E)} - \gamma \mathbf{e}^{(s'_E)}) \right) \right\|_2^2 \right] & \leq \mathbb{E} \left[\frac{2(1+\gamma^2)}{(1-\gamma)^2} \right] \\ & = \frac{2(1+\gamma^2)}{(1-\gamma)^2}. \end{aligned}$$

Hence, we can provide the bound

$$\begin{aligned} \mathbb{E} \left[\left\| \tilde{g}^{(c, \mathbf{u})}((\mathbf{c}, \mathbf{u}), \boldsymbol{\mu}) \right\|_2^2 \right] & \stackrel{(i)}{\leq} 2 \left[32|\mathcal{S}||\mathcal{A}|\alpha^2 + 4 + \frac{2(1+\gamma^2)}{(1-\gamma)^2} \right] \\ & = 64\alpha^2 \cdot |\mathcal{S}||\mathcal{A}| + \frac{4(1+\gamma^2)}{(1-\gamma)^2} + 8. \end{aligned}$$

where in (i) we used $\|\mathbf{x} + \mathbf{y}\|^2 \leq 2(\|\mathbf{x}\|^2 + \|\mathbf{y}\|^2)$. □

Proof of Lemma 2. The unbiasedness follows from

$$\begin{aligned}
\mathbb{E}[\tilde{g}^\mu((\mathbf{c}_t, \mathbf{u}_t), \boldsymbol{\mu}_t)] &= \sum_{s,a,s'} \frac{1}{|\mathcal{S}||\mathcal{A}|} P(s' | s, a) \cdot |\mathcal{S}||\mathcal{A}| \left(c_t(s, a) \mathbf{e}^{(s,a)} - \frac{1}{(1-\gamma)} (u_t(s) \mathbf{e}^{(s,a)} - \gamma u_t(s') \mathbf{e}^{(s,a)}) \right) \\
&= \sum_{s,a} c_t(s, a) \mathbf{e}^{(s,a)} - \frac{1}{(1-\gamma)} \left(\sum_{s,a} u_t(s) \mathbf{e}^{(s,a)} - \gamma \sum_{s,a} \left(\sum_{s'} P(s' | s, a) u_t(s') \right) \mathbf{e}^{(s,a)} \right) \\
&= \mathbf{c}_t - \frac{1}{(1-\gamma)} (\mathbf{B}^\top \mathbf{u} - \gamma \mathbf{P}^\top \mathbf{u}) \\
&= \mathbf{c}_t - \mathbf{T}_\gamma^\top \mathbf{u}.
\end{aligned}$$

For the bound on the maximum entry observe that

$$\begin{aligned}
\|\tilde{g}^\mu((\mathbf{c}_t, \mathbf{u}_t), \boldsymbol{\mu}_t)\|_\infty &= |\mathcal{S}||\mathcal{A}| \max_{s,a,s'} \left\{ \left| c_t(s, a) - \frac{u_t(s) - \gamma u_t(s')}{(1-\gamma)} \right| \right\} \\
&\leq |\mathcal{S}||\mathcal{A}| \left(\|\mathbf{c}_t\|_\infty + \|\mathbf{u}_t\|_\infty \frac{(1+\gamma)}{(1-\gamma)} \right) \\
&= \frac{2|\mathcal{S}||\mathcal{A}|}{(1-\gamma)}
\end{aligned}$$

Finally, the bound on the second-moment can be obtained by:

$$\begin{aligned}
\mathbb{E} \left[\|\tilde{g}^\mu((\mathbf{c}_t, \mathbf{u}_t), \boldsymbol{\mu}_t)\|_{\boldsymbol{\mu}'}^2 \right] &\stackrel{(i)}{\leq} |\mathcal{S}|^2 |\mathcal{A}|^2 \cdot \mathbb{E} \left[2 \|c_t(s, a) \mathbf{e}^{(s,a)}\|_{\boldsymbol{\mu}'}^2 + \frac{4}{(1-\gamma)^2} (\|u_t(s) \mathbf{e}^{(s,a)}\|_{\boldsymbol{\mu}'}^2 + \|\gamma u_t(s') \mathbf{e}^{(s,a)}\|_{\boldsymbol{\mu}'}^2) \right] \\
&= |\mathcal{S}|^2 |\mathcal{A}|^2 \cdot \mathbb{E} \left[\mu'(s, a) \left(2(c_t(s, a))^2 + \frac{4}{(1-\gamma)^2} (u_t(s))^2 + \frac{4\gamma^2}{(1-\gamma)^2} (u_t(s'))^2 \right) \right] \\
&= |\mathcal{S}||\mathcal{A}| \left[\sum_{s,a} \mu'(s, a) \left(2(c_t(s, a))^2 + \frac{4}{(1-\gamma)^2} (u_t(s))^2 \right) \right. \\
&\quad \left. + \sum_{s',s,a} \mu'(s, a) P(s' | s, a) \frac{4\gamma^2}{(1-\gamma)^2} (u_t(s'))^2 \right] \\
&\stackrel{(ii)}{\leq} |\mathcal{S}||\mathcal{A}| \left[\left(2 + \frac{4}{(1-\gamma)^2} \right) \sum_{s,a} \mu'(s, a) + \frac{4\gamma^2}{(1-\gamma)^2} \sum_{s',s,a} \mu'(s, a) P(s' | s, a) \right] \\
&= |\mathcal{S}||\mathcal{A}| \left(2 + \frac{4(1+\gamma^2)}{(1-\gamma)^2} \right),
\end{aligned}$$

where we used $\|\mathbf{x} + \mathbf{y}\|^2 \leq 2[\|\mathbf{x}\|^2 + \|\mathbf{y}\|^2]$ two times for (i) and that $(\mathbf{c}_t, \mathbf{u}_t) \in \mathbb{B}_1^{|\mathcal{S}||\mathcal{A}|} \times \mathbb{B}_1^{|\mathcal{S}|}$ for (ii). \square

A.3 Algorithm convergence

We will follow Jin & Sidford (2020) and show how their results accommodate our problem.

Definition 3 (ℓ_∞ - ℓ_1 convex-concave min-max problem). *Let $f : \mathbb{R}^n \times \mathbb{R}^m \rightarrow \mathbb{R}$ be a differentiable function that is convex in $\mathbf{x} \in \mathbb{R}^n$ and concave in $\mathbf{y} \in \mathbb{R}^m$. We define the ℓ_∞ - ℓ_1 convex-concave min-max problem as*

$$\min_{\mathbf{x} \in \mathbb{B}_\infty^n} \max_{\mathbf{y} \in \Delta^m} f(\mathbf{x}, \mathbf{y}). \tag{3}$$

Furthermore, define the operator

$$G(\mathbf{z}) = G(\mathbf{x}, \mathbf{y}) = [\nabla_{\mathbf{x}} f(\mathbf{x}, \mathbf{y}), -\nabla_{\mathbf{y}} f(\mathbf{x}, \mathbf{y})] = [g^{\mathbf{x}}(\mathbf{x}, \mathbf{y}), g^{\mathbf{y}}(\mathbf{x}, \mathbf{y})].$$

Lemma 4 (cf. Appendix A.1 in Carmon et al. (2019)). *For every $\mathbf{z}_1, \dots, \mathbf{z}_K \in \mathcal{Z} = \mathbb{B}_b^n \times \Delta^m$ it holds that*

$$\text{Gap} \left(\frac{1}{K} \sum_{k=1}^K \mathbf{z}_k \right) \leq \sup_{\mathbf{u} \in \mathcal{Z}} \frac{1}{K} \sum_{k=1}^K \langle G(\mathbf{z}_k), \mathbf{z}_k - \mathbf{u} \rangle.$$

Proof. For all $\mathbf{z} \in \mathcal{Z}$, $f(\mathbf{z}^{\mathbf{x}}, \mathbf{u}^{\mathbf{y}})$ is concave in $\mathbf{u}^{\mathbf{y}}$ and $-f(\mathbf{u}^{\mathbf{x}}, \mathbf{z}^{\mathbf{y}})$ is concave in $\mathbf{u}^{\mathbf{x}}$. Therefore, $\text{gap}(\mathbf{z}, \mathbf{u})$ is concave in \mathbf{u} for every \mathbf{z} and we have

$$\begin{aligned} \text{gap}(\mathbf{z}, \mathbf{u}) &\leq \text{gap}(\mathbf{z}, \mathbf{z}) + \langle \nabla_{\mathbf{u}} \text{gap}(\mathbf{z}, \mathbf{z}), \mathbf{u} - \mathbf{z} \rangle \\ &= \langle \nabla_{\mathbf{u}} \text{gap}(\mathbf{z}, \mathbf{z}), \mathbf{u} - \mathbf{z} \rangle \\ &= \langle -G(\mathbf{z}), \mathbf{u} - \mathbf{z} \rangle \\ &= \langle G(\mathbf{z}), \mathbf{z} - \mathbf{u} \rangle. \end{aligned}$$

Similarly, $\text{gap}(\mathbf{z}; \mathbf{u})$ is convex in \mathbf{z} for every \mathbf{u} . Therefore,

$$\text{gap} \left(\frac{1}{K} \sum_{k=1}^K \mathbf{z}_k; \mathbf{u} \right) \leq \frac{1}{K} \sum_{k=1}^K \text{gap}(\mathbf{z}_k; \mathbf{u}) \leq \frac{1}{K} \sum_{k=1}^K \langle G(\mathbf{z}_k), \mathbf{z}_k - \mathbf{u} \rangle,$$

where the first inequality follows from convexity in \mathbf{z} and the second inequality from the result above. Taking the supremum over the inequality yields the result. \square

The two divergences that we will use in the stochastic mirror descent algorithm for the ℓ_∞ - ℓ_1 convex-concave min-max problem are the following:

1. given the euclidean distance $h(\mathbf{x}) = \frac{1}{2} \|\mathbf{x}\|_2^2$, we obtain the divergence $V_{\mathbf{x}}(\mathbf{x}') = \frac{1}{2} \|\mathbf{x} - \mathbf{x}'\|_2^2$;
2. given $h(\mathbf{y}) = \sum_i y_i \log y_i$, we obtain the Kullback-Leibler divergence $V_{\mathbf{y}}(\mathbf{y}') = \sum y_i \log \left(\frac{y'_i}{y_i} \right)$.

Theorem 3 (c.f. Theorem 3 (Jin & Sidford, 2020)). *Given a ℓ_∞ - ℓ_1 convex-concave-min-max problem (3), desired accuracy ϵ , $(v^{\mathbf{x}}, \|\cdot\|_2)$ -bounded estimators $\tilde{g}^{\mathbf{x}}$ of $g^{\mathbf{x}}$, and $(\frac{2v^{\mathbf{y}}}{\epsilon}, v^{\mathbf{y}}, \|\cdot\|_{\Delta^m})$ -bounded estimators $\tilde{g}^{\mathbf{y}}$ of $g^{\mathbf{y}}$. Algorithm 1 with choice of parameters $\eta_{\mathbf{x}} \leq \frac{\epsilon}{4v^{\mathbf{x}}}$, $\eta_{\mathbf{y}} \leq \frac{\epsilon}{4v^{\mathbf{y}}}$ outputs an expected ϵ -approximate optimal solution within any iteration number $T \geq \max\left\{ \frac{16nb^2}{\epsilon\eta_{\mathbf{x}}}, \frac{8\log(m)}{\epsilon\eta_{\mathbf{y}}} \right\}$.*

Proof. Note that $V_{\mathbf{x}}$ is 1-strongly convex. Since $\eta_{\mathbf{y}} \leq \frac{\epsilon}{4v^{\mathbf{y}}}$, we have that

$$\|\eta^{\mathbf{y}} \tilde{g}_t^{\mathbf{y}}\|_\infty \leq \frac{\epsilon}{4v^{\mathbf{y}}} \cdot \|\tilde{g}_t^{\mathbf{y}}\|_\infty \leq \frac{\epsilon}{4v^{\mathbf{y}}} \cdot \frac{2v^{\mathbf{y}}}{\epsilon} = \frac{1}{2}.$$

Hence, by Lemma 1 and Lemma 2 in Jin & Sidford (2020) we know that

$$\begin{aligned} \sum_{t \in [T]} \langle \eta^{\mathbf{x}} \tilde{g}_t^{\mathbf{x}}, \mathbf{x}_t - \mathbf{x} \rangle &\leq V_{\mathbf{x}_1}(\mathbf{x}) + \frac{\eta^{\mathbf{x}2}}{2} \sum_{t \in [T]} \|\tilde{g}_t^{\mathbf{x}}\|_2^2, \\ \sum_{t \in [T]} \langle \eta^{\mathbf{y}} \tilde{g}_t^{\mathbf{y}}, \mathbf{y}_t - \mathbf{y} \rangle &\leq V_{\mathbf{y}_1}(\mathbf{y}) + \frac{\eta^{\mathbf{y}2}}{2} \sum_{t \in [T]} \|\tilde{g}_t^{\mathbf{y}}\|_{\mathbf{y}_t}^2. \end{aligned}$$

Now, define $\hat{g}_t^{\mathbf{x}} := g_t^{\mathbf{x}} - \tilde{g}_t^{\mathbf{x}}$, $\hat{g}_t^{\mathbf{y}} := g_t^{\mathbf{y}} - \tilde{g}_t^{\mathbf{y}}$, and the sequences $\hat{\mathbf{x}}_1, \dots, \hat{\mathbf{x}}_T$ and $\hat{\mathbf{y}}_1, \dots, \hat{\mathbf{y}}_T$ by

$$\begin{aligned} \hat{\mathbf{x}}_1 &= \mathbf{x}_1, \quad \hat{\mathbf{x}}_{t+1} = \arg \min_{\mathbf{x} \in \mathbb{B}_b^n} \langle \eta^{\mathbf{x}} \hat{g}_t^{\mathbf{x}}, \mathbf{x} \rangle + V_{\hat{\mathbf{x}}_t}(\mathbf{x}), \\ \hat{\mathbf{y}}_1 &= \mathbf{y}_1, \quad \hat{\mathbf{y}}_{t+1} = \arg \min_{\mathbf{y} \in \Delta^m} \langle \eta^{\mathbf{y}} \hat{g}_t^{\mathbf{y}}, \mathbf{y} \rangle + V_{\hat{\mathbf{y}}_t}(\mathbf{y}). \end{aligned}$$

In a similar way to $\eta^{\mathbf{y}} g_t^{\mathbf{y}}$, we can bound the ℓ_∞ -norm of $\eta^{\mathbf{y}} \hat{g}_t^{\mathbf{y}}$

$$\|\eta^{\mathbf{y}} \hat{g}_t^{\mathbf{y}}\|_\infty \leq \|\eta^{\mathbf{y}} \tilde{g}_t^{\mathbf{y}}\|_\infty + \|\eta^{\mathbf{y}} g_t^{\mathbf{y}}\|_\infty = \|\eta^{\mathbf{y}} \tilde{g}_t^{\mathbf{y}}\|_\infty + \|\mathbb{E}[\eta^{\mathbf{y}} \tilde{g}_t^{\mathbf{y}}]\|_\infty \leq 2\|\eta^{\mathbf{y}} \tilde{g}_t^{\mathbf{y}}\|_\infty \leq 1.$$

Therefore, using the lemmas as above we get

$$\begin{aligned} \sum_{t \in [T]} \langle \eta^{\mathbf{x}} \hat{g}_t^{\mathbf{x}}, \mathbf{x}_t - \mathbf{x} \rangle &\leq V_{\mathbf{x}_1}(\mathbf{x}) + \frac{\eta^{\mathbf{x}2}}{2} \sum_{t \in [T]} \|\hat{g}_t^{\mathbf{x}}\|_2^2, \\ \sum_{t \in [T]} \langle \eta^{\mathbf{y}} \hat{g}_t^{\mathbf{y}}, \mathbf{y}_t - \mathbf{y} \rangle &\leq V_{\mathbf{y}_1}(\mathbf{y}) + \frac{\eta^{\mathbf{y}2}}{2} \sum_{t \in [T]} \|\hat{g}_t^{\mathbf{y}}\|_{\mathbf{y}_t}^2. \end{aligned}$$

Since $g_t^{\mathbf{x}} = \hat{g}_t^{\mathbf{x}} + \tilde{g}_t^{\mathbf{x}}$ and $g_t^{\mathbf{y}} = \hat{g}_t^{\mathbf{y}} + \tilde{g}_t^{\mathbf{y}}$,

$$\begin{aligned} &\sum_{t \in [T]} [\langle g_t^{\mathbf{x}}, \mathbf{x}_t - \mathbf{x} \rangle + \langle g_t^{\mathbf{y}}, \mathbf{y}_t - \mathbf{y} \rangle] \\ &= \sum_{t \in [T]} \left[\frac{1}{\eta^{\mathbf{x}}} \langle \eta^{\mathbf{x}} \tilde{g}_t^{\mathbf{x}}, \mathbf{x}_t - \mathbf{x} \rangle + \frac{1}{\eta^{\mathbf{y}}} \langle \eta^{\mathbf{y}} \tilde{g}_t^{\mathbf{y}}, \mathbf{y}_t - \mathbf{y} \rangle \right] + \sum_{t \in [T]} \left[\frac{1}{\eta^{\mathbf{x}}} \langle \eta^{\mathbf{x}} \hat{g}_t^{\mathbf{x}}, \hat{\mathbf{x}}_t - \mathbf{x} \rangle + \frac{1}{\eta^{\mathbf{y}}} \langle \eta^{\mathbf{y}} \hat{g}_t^{\mathbf{y}}, \hat{\mathbf{y}}_t - \mathbf{y} \rangle \right] \\ &+ \sum_{t \in [T]} [\langle \hat{g}_t^{\mathbf{x}}, \mathbf{x}_t - \hat{\mathbf{x}}_t \rangle + \langle \hat{g}_t^{\mathbf{y}}, \mathbf{y}_t - \hat{\mathbf{y}}_t \rangle] \\ &= \frac{1}{\eta^{\mathbf{x}}} \sum_{t \in [T]} [\langle \eta^{\mathbf{x}} \tilde{g}_t^{\mathbf{x}}, \mathbf{x}_t - \mathbf{x} \rangle] + \frac{1}{\eta^{\mathbf{x}}} \sum_{t \in [T]} [\langle \eta^{\mathbf{x}} \hat{g}_t^{\mathbf{x}}, \hat{\mathbf{x}}_t - \mathbf{x} \rangle] + \frac{1}{\eta^{\mathbf{y}}} \sum_{t \in [T]} [\langle \eta^{\mathbf{y}} \tilde{g}_t^{\mathbf{y}}, \mathbf{y}_t - \mathbf{y} \rangle] \\ &+ \frac{1}{\eta^{\mathbf{y}}} \sum_{t \in [T]} [\langle \eta^{\mathbf{y}} \hat{g}_t^{\mathbf{y}}, \hat{\mathbf{y}}_t - \mathbf{y} \rangle] + \sum_{t \in [T]} [\langle \hat{g}_t^{\mathbf{x}}, \mathbf{x}_t - \hat{\mathbf{x}}_t \rangle + \langle \hat{g}_t^{\mathbf{y}}, \mathbf{y}_t - \hat{\mathbf{y}}_t \rangle] \\ &\leq \frac{2}{\eta^{\mathbf{x}}} V_{\mathbf{x}_1}(\mathbf{x}) + \frac{\eta^{\mathbf{x}}}{2} \sum_{t \in [T]} [\|\tilde{g}_t^{\mathbf{x}}\|_2^2 + \|\hat{g}_t^{\mathbf{x}}\|_2^2] + \sum_{t \in [T]} \langle \hat{g}_t^{\mathbf{x}}, \mathbf{x}_t - \hat{\mathbf{x}}_t \rangle \\ &+ \frac{2}{\eta^{\mathbf{y}}} V_{\mathbf{y}_1}(\mathbf{y}) + \frac{\eta^{\mathbf{y}}}{2} \sum_{t \in [T]} [\|\tilde{g}_t^{\mathbf{y}}\|_{\mathbf{y}_t}^2 + \|\hat{g}_t^{\mathbf{y}}\|_{\mathbf{y}_t}^2] + \sum_{t \in [T]} \langle \hat{g}_t^{\mathbf{y}}, \mathbf{y}_t - \hat{\mathbf{y}}_t \rangle. \end{aligned}$$

Consider the operator $G(\mathbf{z}) := [g^{\mathbf{x}}(\mathbf{x}, \mathbf{y}), -g^{\mathbf{y}}(\mathbf{x}, \mathbf{y})]$. As min-max problem 3 is convex in its first argument and concave in its second argument, by Lemma 4, if we show that

$$\sup_{\mathbf{u} \in \mathcal{Z}} \frac{1}{T} \sum_{t \in [T]} \langle G(\mathbf{z}_t), \mathbf{z}_t - \mathbf{u} \rangle \leq \epsilon,$$

we obtain that $\text{Gap}(\frac{1}{T} \sum_{t=1}^T \mathbf{z}_t) \leq \epsilon$. Now take the expectation on both sides:

$$\begin{aligned}
\mathbb{E} \sup_{\mathbf{u} \in \mathcal{Z}} \frac{1}{T} \sum_{t \in [T]} \langle G(\mathbf{z}_t), \mathbf{z}_t - \mathbf{u} \rangle &= \mathbb{E} \frac{1}{T} \sup_{(\mathbf{x}, \mathbf{y})} \left[\sum_{t \in [T]} \langle g^{\mathbf{x}}(\mathbf{x}, \mathbf{y}), \mathbf{x}_t - \mathbf{x} \rangle + \sum_{t \in [T]} \langle g^{\mathbf{y}}(\mathbf{x}, \mathbf{y}), \mathbf{y}_t - \mathbf{y} \rangle \right] \\
&\stackrel{(i)}{\leq} \frac{1}{T} \mathbb{E} \sup_{(\mathbf{x}, \mathbf{y})} \left[\frac{2}{\eta^{\mathbf{x}}} V_{\mathbf{x}_1}(\mathbf{x}) + \frac{\eta^{\mathbf{x}}}{2} \sum_{t \in [T]} [\|\tilde{g}_t^{\mathbf{x}}\|_2^2 + \|\hat{g}_t^{\mathbf{x}}\|_2^2] \right. \\
&\quad \left. + \frac{2}{\eta^{\mathbf{y}}} V_{\mathbf{y}_1}(\mathbf{y}) + \frac{\eta^{\mathbf{y}}}{2} \sum_{t \in [T]} [\|\tilde{g}_t^{\mathbf{y}}\|_2^2 + \|\hat{g}_t^{\mathbf{y}}\|_2^2] \right] \\
&\stackrel{(ii)}{\leq} \frac{1}{T} \mathbb{E} \sup_{(\mathbf{x}, \mathbf{y})} \left[\frac{2}{\eta^{\mathbf{x}}} V_{\mathbf{x}_1}(\mathbf{x}) + \eta^{\mathbf{x}} \sum_{t \in [T]} \|\tilde{g}_t^{\mathbf{x}}\|_2^2 + \frac{2}{\eta^{\mathbf{y}}} V_{\mathbf{y}_1}(\mathbf{y}) + \eta^{\mathbf{y}} \sum_{t \in [T]} \|\tilde{g}_t^{\mathbf{y}}\|_2^2 \right] \\
&\stackrel{(iii)}{\leq} \sup_{\mathbf{x}} \frac{2}{\eta^{\mathbf{x}} T} V_{\mathbf{x}_1}(\mathbf{x}) + \eta^{\mathbf{x}} v^{\mathbf{x}} + \sup_{\mathbf{y}} \frac{2}{\eta^{\mathbf{y}} T} V_{\mathbf{y}_1}(\mathbf{y}) + \eta^{\mathbf{y}} v^{\mathbf{y}} \\
&\stackrel{(iv)}{\leq} \frac{4nb^2}{\eta^{\mathbf{x}} T} + \eta^{\mathbf{x}} v^{\mathbf{x}} + \frac{2 \log m}{\eta^{\mathbf{y}} T} + \eta^{\mathbf{y}} v^{\mathbf{y}} \\
&\stackrel{(v)}{\leq} \epsilon,
\end{aligned}$$

where in (i) we used that $\mathbb{E}[\langle \hat{g}_t^{\mathbf{x}}, \mathbf{x}_t - \hat{\mathbf{x}}_t \rangle \mid 1, \dots, T] = \mathbb{E}[\langle \hat{g}_t^{\mathbf{y}}, \mathbf{y}_t - \hat{\mathbf{y}}_t \rangle \mid 1, \dots, T] = 0$; (ii) $\mathbb{E}[\|\hat{g}_t^{\mathbf{x}}\|_2^2] \leq \mathbb{E}[\|\tilde{g}_t^{\mathbf{x}}\|_2^2]$ and $\mathbb{E}[\sum_i [\hat{y}_t]_i [\hat{g}_t^{\mathbf{y}}]_i^2] \leq \mathbb{E}[\sum_i [\hat{y}_t]_i [\tilde{g}_t^{\mathbf{y}}]_i^2]$ due to $\mathbb{E}[(X - \mathbb{E}[X])^2] \leq \mathbb{E}[X^2]$; (iii) due to the assumptions on the estimators; (iv) by properties of KL-divergence and that $\frac{1}{2} \|\mathbf{x} - \mathbf{x}_0\|_2^2 \leq 2nb^2$; (v) the choice of $\eta^{\mathbf{x}} = \frac{\epsilon}{4v^{\mathbf{x}}}$, $\eta^{\mathbf{y}} = \frac{\epsilon}{4v^{\mathbf{y}}}$, and $T \geq \max\{\frac{16nb^2}{\epsilon\eta^{\mathbf{x}}}, \frac{8 \log m}{\epsilon\eta^{\mathbf{y}}}\}$. \square

Now, Theorem 2 follows directly from the bounds of the gradient estimators and Theorem 3.

B Numerical experiments

B.1 Gridworld

We extend the analysis to Gridworld environments with four random obstacle-goal configurations to assess the method's applicability to arbitrary cost structures. We retain the experimental setup described in Section 5.2, fixing the regularization parameter to $\alpha = 0.005$ and generating a suboptimal expert via early solver termination. For each configuration, we compare the resulting apprentice policy against both the optimal and expert policies, and examine the learned cost vector for the action "down" relative to the ground truth given by the color coding of the policies' grid.

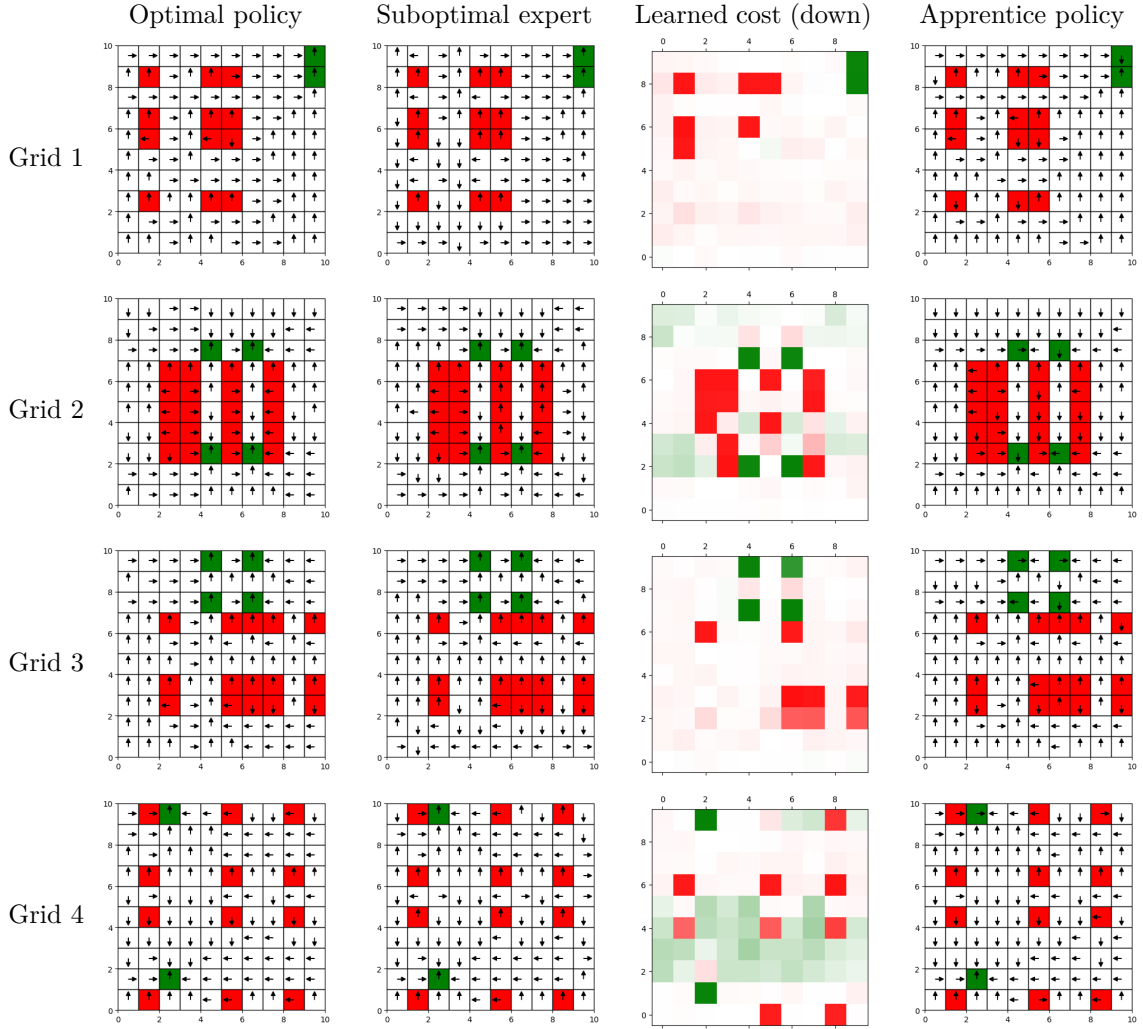


Figure 16: Effect of the regularization on the cost vector.